Accelerating loss of resilience in Bornean rainforests

Shujie Chang[1,3,4*], Neel Patrick Le Penru[1,2*], Robert M. Ewers[1]

[1] Georgina Mace Centre for the Living Planet, Department of Life Sciences, Imperial College London, Ascot, UK
[2] Dyson School of Design Engineering, Imperial College London, London, UK
[3] Department of Zoology, University of Cambridge, Cambridge, UK
[4] University Museum of Zoology, University of Cambridge, Cambridge, UK

[*] Corresponding authors:
Shujie Chang: sc2535@cam.ac.uk
Neel Le Penru: neel.le-penru16@imperial.ac.uk

Abstract

Tropical rainforest resilience is being eroded by climate change and human activity, potentially risking tipping points of mass forest dieback towards Savannah-like or treeless states. Recent work on the Amazon used decades of satellite-derived vegetation data to reveal increases in generic early-warning signals of a bifurcation-induced tipping point, which were most pronounced in areas with less rainfall and closer to human activity. Here, we extend this approach to Borneo and include novel considerations to assess if, when and how rapidly resilience loss has accelerated, and whether that acceleration has any relationship with biodiversity. We detected a direct signal of resilience loss through the critical slowing down of Bornean rainforest's response to perturbations, which was observed through rising lag-1 autocorrelation and variance of long-term satellite-sensed vegetation data. We find Bornean rainforest lost resilience over our full study period (from 1991-2016), with a marked increase in the rate of loss from 2006. Resilience loss was most severe and accelerated earlier in subregions with lower precipitation, lower biodiversity, higher temperature and higher human activity, although this pattern was disrupted post-2006 since when resilience loss has been faster in areas with higher precipitation and lower human activity. Overall, we provide evidence of Bornean rainforest resilience loss, underscoring the urgent need for ecosystem conservation and climate change mitigation within Borneo and worldwide.

Introduction

Tropical rainforests are essential for global biodiversity and ecosystem services, supporting over two-thirds of the world's terrestrial biodiversity and providing critical functions in climate regulation, water cycling, and carbon sequestration (Ferraz et al., 2014; Gardner et al., 2009; Houghton et al., 2015; Pan et al., 2011; Shimamoto et al., 2018). However, over the past few decades, tropical regions have experienced some of the most severe forest loss (Achard et al., 2002; Hansen et al., 2013). Borneo specifically has lost considerable forest to drought, fire, deforestation, and other pressures (Achard et al., 2002; Curran et al., 2004; Gaveau et al., 2016; Hansen et al., 2013; Langner & Siegert, 2009). Worryingly, there are concerns and mounting evidence that climate and land-use change are driving tropical forests towards tipping points that would see mass forest dieback resulting in alternative Savannah-like or treeless stable states (Boulton et al., 2022; Flores et al. 2024; Hirota et al. 2011; Lenton et al. 2022; Verbesselt et al., 2016). The threat of tipping

points is particularly alarming as they can be especially difficult to reverse and their approach cannot be inferred from gradual changes to the mean state of the system alone (Boers, 2021; Lenton et al., 2022; Scheffer et al., 2009; Smith et al., 2023). In this article, we build on existing work using satellite data to track resilience-based early-warning signals of tipping points in global vegetation, including tropical forests, to more closely examine trends in Bornean rainforest resilience loss and its possible drivers.

Resilience, broadly defined as a system's ability to withstand perturbations, is generally thought to decline prior to a state shift. Ways to interpret and measure resilience vary within ecology and across disciplines, though. Many ecologists follow Holling's notion of 'ecological resilience', which considers resilience as the amount of perturbation an ecosystem can absorb without changing its function, in contrast to 'engineering resilience', defined as a system's recovery rate from perturbation (Holling, 1973, 1996). Under the view of ecosystems as complex dynamical systems, resistance and recovery are fundamentally linked, as both are determined by the strength of restorative negative feedback that maintains the system at equilibrium, λ (defined mathematically by the system's dominant eigenvalue). More specifically, λ is inversely proportional to the system's recovery rate from small perturbations (Pimm, 1984; Scheffer et al., 2009; Wissel, 1984). It also locally approximates the second derivative of the system's potential landscape – a function in which stable equilibria are local minima, sometimes termed 'basins of attraction', whose shape and size determine various features of ecological resilience including the amount of perturbation required to push the system from one stable state to another (Dakos & Kéfi, 2022).

Tipping points are qualitative changes to the state of system in response to small perturbations or increments in conditions (Lenton et al., 2008). Though they may be brought about by various mechanisms (Dakos et al., 2024), tipping points are commonly associated with bifurcations, in particular fold (a.k.a. saddle-node or catastrophic) bifurcations in which stabilising negative feedback breaks down, triggering an abrupt shift to an alternate stable state driven by positive feedback (Boulton et al., 2017; Jones et al., 2009; Scheffer et al., 2001, 2009). As a fold bifurcation approaches, λ approaches zero and the system thus recovers more slowly from perturbations – a phenomenon known as 'critical slowing down' (CSD; Strogatz, 1994; van Nes & Scheffer, 2007; Wissel, 1984). The basin of attraction also becomes shallower. Hence, resilience is lost. Moreover,

the current state of the system is more likely to resemble its past states and to accumulate more extreme fluctuations over time. This pattern is typically reflected in increased lag-1 autocorrelation (AC(1)) and variance, which are two classical early-warning signals of resilience loss ahead of a tipping point (Carpenter & Brock, 2006; Dakos et al., 2008; Ives, 1995, Scheffer 2009).

While other methods to monitor resilience loss and critical transitions have been proposed (for overviews see Clements & Ozgul, 2018; Dakos et al., 2024; Dakos & Kéfi, 2022), early-warning signals based on statistical properties of a system's fluctuations about its long-term mean remain prominent, thanks to their generic nature stemming from the behaviour of complex dynamical systems. Statistical early-warning signals have been observed in a wide range of natural systems in long timeseries of the system state or along spatial stress/disturbance gradients. These include yeast population collapses and extinctions of *Daphnia magnum* in laboratory experiments (Dai et al., 2012; Drake & Griffen, 2010), regime changes in food webs and lake eutrophication in aquatic ecosystems (Carpenter et al., 2011; Wang et al., 2012), and even environment-scale systems such as the melting of the Greenland ice sheet and the collapse of the Atlantic Meridional Overturning Circulation (Boers, 2021; Boers & Rypdal, 2021).

For forests and the biosphere at large, satellite data has proven an invaluable tool for tracking early-warning signals in vegetation features (e.g., biomass, water content) on the scale of decades at high spatiotemporal resolution (Lenton et al., 2022; Verbesselt et al., 2016). While this work has revealed worrying global trends in forest resilience loss, more detailed analyses of these trends, such as identifying potential drivers of resilience loss (Boulton et al., 2022) and examining alternative stable states empirically (Hirota et al., 2011, Flores et al., 2024) have focused primarily on the Amazon rainforest. In particular, Boulton et al. (2022) revealed a marked loss of Amazon rainforest resilience from the early 2000s, with faster loss in regions with lower mean annual precipitation and greater proximity to human activity, as measured by how consistently AC(1) and variance increased in those areas (based on Kendall τ correlation coefficient).

While external factors of forest resilience loss, such as climate and human activities, have primarily been investigated, internal ecological drivers, particularly biodiversity, have received less attention. Although previous studies have demonstrated the importance of biodiversity in supporting ecosystem resilience, most empirical analyses have focused on community-level processes and

interactions (Coux et al., 2016; Elmqvist et al., 2003; Mouillot et al., 2013). Relatively little work has to-date empirically explored whether and how biodiversity relates to nonlinear dynamical system models of ecosystems, though the relationship of biodiversity to ecosystem stability has long been a topic of interest in ecology (e.g., May, 1972; Pimm, 1984; Kéfi et al., 2019).

Here, we move away from the Amazon rainforest and adapt the methods used by Boulton et al. (2022) to quantify the changing resilience of tropical forest across Borneo. We measure the AC(1) and variance of satellite-sensed vegetation data for Borneo – incorporating recent advice on aggregating satellite data with sensor shifts (Smith et al., 2023) – and use breakpoint regression to provide additional quantitative metrics for the onset time and magnitude of pronounced increases in these early-warning signals. We also consider a broader set of regional factors that may be driving rainforest resilience loss: precipitation, temperature, human activity and animal biodiversity. Through our analysis, we provide more detailed insight into patterns of resilience loss in Bornean rainforest and the factors that may be underpinning or associated with it. We also expand the toolkit for interpreting early-warning signals of critical transitions to explicitly quantify the timing and magnitude of resilience loss.

Results

Resilience Change

We quantified the change in resilience of rainforest across Borneo for the period 1991 to 2016 focusing on 475 grid cells (0.25° × 0.25°) identified as intact rainforest, based on high forest cover and absence of human land use (Methods) as in previous work (Boulton et al., 2022). We calculated two early-warning signals of a critical transition, AC(1) and variance, in sliding windows on detrended vegetation optical depth (VOD) time series (Methods). As AC(1) has been shown to be a more robust indicator than variance (Boulton et al., 2013; Dakos, van Nes, et al., 2012), we primarily focused on AC(1) in our analyses, with variance serving as a supplementary metric to confirm that patterns in AC(1) likely stem from changes in ecosystem resilience (Smith et al., 2023; Methods). We then applied breakpoint regression to the AC(1) time series and calculated the following three metrics of resilience change. First, the consistency of resilience loss, measured by the AC(1) Kendall τ (as in previous work) for both the post-breakpoint period and the full time

series. Second, the timing of the breakpoint. Third, the magnitude of resilience loss, measured by the slope of linear regressions fit to both the post-breakpoint period and to the full AC(1) time series. We also sometimes consider Δslope, the difference in the slope of linear regressions applied to the post- and pre-breakpoint AC(1) time series.

Across Borneo, there was an upward trend in the mean AC(1) time series throughout the study period (Fig. 1; $\tau = 0.719$), indicating a consistent reduction in rainforest resilience. A breakpoint occurred around March 2006 (95% CI: February 2006–March 2006), after which the long-term upward trend became more pronounced (prior to breakpoint: $\tau = 0.374$, slope = 1.80×10^{-5}; post breakpoint: $\tau = 0.661$, slope = 6.22×10^{-5}; Fig. 1). The timing of the breakpoint did not align with any changes in the mix of satellite sensors used to measure VOD that occurred during the study period, indicating it was unlikely to be an artefact of instrumental transitions (Methods; Supplementary Fig. 1).

Most individual grid cells (82%; mean breakpoint = December 2003 ± 31 months) exhibited breakpoints earlier than that observed for the entire study area (Fig. 2a, b). In other words, the large-scale signal of resilience loss in Borneo appeared after most subregions had already experienced an increase in the loss of resilience. After passing the breakpoint, a majority of grid cells (61%) within the study area experienced an increase in AC(1), especially in the northwest coastal and central-southern regions (Fig. 2c, d), where resilience loss was most consistent. The Δslope values for individual grid cells were strongly correlated with Kendall τ (Spearman's $\rho = 0.725$, $p < 0.001$), with 59% of the study area showing positive values (Fig. 2e, f) and the overall distribution significantly greater than zero (t-test: $p < 0.001$). Thus, most of Borneo experienced a higher rate of resilience loss post-breakpoint.

These results are robust to the use of varying broadleaf forest cover thresholds to determine the study area (Supplementary Figs. 2, 3) and different window lengths to estimate AC(1) (Supplementary Fig. 4). Analysis using variance as a resilience indicator also revealed an increased trend (Supplementary Fig. 5) and the post-2006 time series of AC(1) and variance were strongly correlated (Spearman's $\rho = 0.594$, $p < 0.001$), indicating that the changes in the resilience indicators were most likely due to actual resilience loss (Smith et al., 2023).

To make a direct, like-for-like comparison with the Amazon, we recalculated the VOD AC(1) result in Boulton et al. (2022) using our processing pipeline (Methods; Supplementary Fig.6). The AC(1) time series for the Amazon still shows an increasing trend after the breakpoint ($\tau = 0.448$, slope = 2.18×10^{-5}), though the timing of the breakpoint changed slightly with our analyses from January 2000 (95% CI: November 1999–March 2000; Boulton et al., 2023) to September 2001 (95% CI: June 2001–December 2001; Supplementary Fig.6a). Across the Amazon, most individual grid cells showed a change in their resilience trend later than the change for the overall area (Supplementary Fig. 6b, c), possibly indicating different mechanisms driving resilience loss compared to Borneo, where most grid cells showed declining resilience before the signal emerged for the aggregate area. Moreover, the Amazon overall showed gains in resilience (declining AC(1) and variance) before its breakpoints, whereas the data for Borneo show resilience loss throughout the whole study period (though it increased post-breakpoint).

Factors Correlated with Resilience Change

To explore how climate, human activity and biodiversity may be associated with the resilience of Bornean rainforests, we quantified the correlations between our resilience metrics and four factors: mean annual precipitation, mean annual temperature, human footprint and vertebrate species richness (amphibians, birds, mammals and reptiles; Methods). Correlations between the factors themselves were weak, showing no confounding effects between them (Supplementary Fig. 7). Linear models directly applied using individual grid cells as replicates to explore the relationships between resilience and these factors showed mostly non-significant results with low explanatory power (Supplementary Table 1), indicating that ecosystem resilience is influenced by multiple factors interacting through complex processes. Therefore, as in previous work (Boulton et al., 2022; Verbesselt et al., 2016), we employed sliding bands of grid cells to aggregate those with similar values of each factor. This procedure minimizes the noise of other factors and captures the resilience change for numerous subsets of regions along a gradient of each factor (e.g., sliding bands of subsets of regions with increasing precipitation; see Methods).

Over the whole study period, areas with lower precipitation had an earlier onset of increased resilience loss (Fig. 3a), with more consistent and stronger declines overall (red lines, Fig. 3b, c). However, higher precipitation areas had more consistent and stronger resilience loss post-

breakpoint (blue lines, Fig. 3b, c). Temperature had a variable and overall minimal impact on all three metrics (Fig. 3d-f). Breakpoints were earliest for regions at the extremes of Borneo's temperature range, with the earliest occurring in grid cells sharing high temperatures (Fig. 3d). Trends between temperature and the consistency and magnitude of resilience loss were generally weak, with the strongest being a slight but clear positive linear trend with the rate of resilience loss (slope) over the whole study period (red line, Fig. 3f). Areas with more intensive human activity tended to undergo increased resilience loss earlier (Fig. 3g) and faced more pronounced resilience loss over the whole study period (red lines, Fig 3h, i). But, post-breakpoint, high human footprint areas had less consistent and a lower rate of resilience loss (blue lines, Fig 3h, i).

Areas of high biodiversity tended to experience an increased rate in resilience loss slightly later (Fig. 3j), with slightly less resilience having been lost across the whole study period (red lines, Fig. 3k, l) and markedly less consistent and strong resilience loss post-breakpoint (blue lines, Fig. 3k, l). The biodiversity patterns were generally consistent across each taxon, though over the full study period each taxon presented a very weak positive trend between the number of species and consistency of resilience loss (Supplementary Fig. 8b, e, h, k). Grid cells sharing more species of amphibians lost more resilience than those with fewer species (Supplementary Fig. 8c). We also note that the data for individual taxa were very variable (more so than for overall biodiversity) and often presented weak trends and/or linear regressions with low adjusted R-squared values. In addition, the species richness of individual taxa exhibited varying degrees of correlation (Supplementary Fig. 9). The above patterns for all factors were robust to our choice of band size for the analyses, with the exception of mammal species richness (Supplementary Figs. 10, 11). Contrary to the general trends for biodiversity and the band size in Fig. 3 and Supplementary Fig. 8, in analysis with fewer cells per band areas with lower mammal species richness displayed earlier breakpoints and higher magnitude resilience loss (Supplementary Fig. 11g, i).

Discussion

Our study has found that, similarly to the Amazon (Boulton et al., 2022), Bornean rainforests are losing resilience. However, differences in the timing of increased resilience loss (breakpoints in AC(1) and variance) between these two regions suggests that this widespread phenomenon is likely

driven by regional factors and/or local responses to global climatic events. Unlike the Amazon's reversal from resilience gain to resilience loss that occurred around 2001, Bornean rainforest experienced continuous resilience loss throughout the study period (i.e., from the early 1990s), with an accelerated decline after 2006. The average rate of resilience loss in Borneo also appears to surpass that of the Amazon, suggesting tipping points may be more imminent in Southeast Asia than in the Amazon.

Further differences emerge when comparing the temporal patterns of resilience breakpoints identified at landscape versus local scales. In Borneo, local-scale (individual grid cell) breakpoints generally preceded the overall breakpoint, suggesting that the Borneo-wide acceleration of resilience loss may have been the product of accumulated local resilience loss. Conversely, in the Amazon, local-scale breakpoints typically occurred after the overall breakpoint. This may be due to regional-scale drivers — particularly severe climatic events such as widespread droughts — directly impacting large areas. It may also be that gradual resilience loss in influential subregions of the Amazon have impacts that propagate spatially to exert a wider impact over broad areas of forest. For instance, deforestation in upwind regions may reduce evapotranspiration with severe consequences for downwind forests that could lose an important share of their precipitation as a result (Staal et al., 2018).

Despite Borneo showing a loss of resilience across its entire area and within most subregions, we found that there were still a number of individual cells that did not lose resilience or even appear to have gained it. This spatial heterogeneity reveals the complexity of resilience and the importance of scale in our results. While our analyses provide some insights into underlying mechanisms of resilience loss through correlations with possible explanatory factors, the existence of areas that deviate from the general trend suggests these might make important locations in which to focus future research. Understanding why these locations perform well could provide valuable insights into the mechanisms that support rainforest resilience.

Across Borneo, we found that areas with lower precipitation lost more resilience over the full study period, which is broadly comparable to prior findings (Boulton et al., 2022; Flores et al., 2024; Verbesselt et al., 2016). However, we identified unique nuances to this relationship: the onset of increased resilience loss occurred later in wetter regions with more severe resilience loss after the

breakpoint. Drier tropical forests have been shown to exhibit lower functional diversity and experience declining functional redundancy with increasing soil water and vapor pressure deficits (Aguirre-Gutiérrez et al., 2022), which may predispose these areas to earlier resilience thresholds. The subsequent, more pronounced post-breakpoint resilience loss in wetter regions may result from breaching thresholds in feedback that typically sustain resilience under wetter conditions, leading to a more rapid and pronounced deterioration once these mechanisms fail. However, further investigation is required to clarify whether this is the case.

Though trends between temperature and our resilience metrics were not strong, those that were clearest broadly agree with prior findings that higher temperatures correlate with greater loss of resilience (Verbesselt et al., 2016). This pattern can be partly attributed to heat stress, which exacerbates evapotranspiration, reduces photosynthetic efficiency, and increases susceptibility to pests or diseases, ultimately weakening ecosystem resilience (Allen et al., 2010; Trumbore et al., 2015).

Regarding human activity, intense human footprints were associated with more pronounced loss of resilience overall, as was observed in the Amazon (Boulton et al., 2022). This likely occurs through fires, pollution and potentially logging and deforestation (though we note our study area focussed on areas of high tree cover in 2001 with no human land use, see Methods). Furthermore, in areas with higher human impact, the accelerated rate of resilience loss tended to occur earlier, though the subsequent post-breakpoint resilience loss was of lower consistency and magnitude than low human footprint areas. In rainforest ecosystems experiencing extensive human intervention, key ecological processes (e.g., seed dispersal and pollination) and networks are disrupted, making these systems more vulnerable to disturbances (Morris, 2010; Neuschulz et al., 2016). Fires and deforestation can also produce a drier microclimate that makes it easier for subsequent fires to start and spread (Lenton et al., 2024; Staal et al., 2018). There is potential that positive human influences, such as reforestation and forest restoration efforts, might contribute to the lower rate of resilience loss in areas of high human footprint after 2006, though this interpretation would require considerable further investigation before it could be made with any degree of certainty.

We found that areas with higher species richness experienced less resilience loss, especially after the breakpoint. This pattern appeared for overall animal biodiversity and, broadly, within individual

animal taxa. Exceptions in some individual taxa (Supplementary Fig. 8) and for smaller band sizes (Supplementary Fig. 11) may simply be due to more prevalent noise in these smaller subsets of data. On a more fundamental level, an obvious debate is whether it is driven by animal biodiversity strengthening the resilience of rainforests in a causative manner, or simply an artefactual correlation. Previous research indicates that high species richness enhances functional diversity, allowing disturbances to be partitioned or mitigated through asynchronous and variable species responses, while functional redundancy ensures that ecosystem processes remain intact when certain species are threatened, ultimately bolstering overall resilience (Loreau & de Mazancourt, 2013; Mouillot et al., 2013; Oliver et al., 2015a, 2015b). On the other hand, although short-term resilience loss might not immediately trigger a regime shift, it may manifest in more subtle ecosystem impacts (e.g., leaf wilting, fruit scarcity), prompting animals to migrate to more resilient areas in search of resources. However, given the nature of the biodiversity data used here, aggregated over decades and lacking population-level resolution, we cannot conclusively disentangle the mechanisms behind these patterns. This underscores the need for exploring new and existing field-based studies, be they manual or based on autonomous monitoring technologies, such as acoustics and camera traps, to better clarify how biodiversity and resilience interact.

By introducing two additional metrics (breakpoint and slope) of resilience change, we captured more detail on the correlates and potential drivers of resilience loss in Southeast Asian rainforest. We emphasize the analysis is correlational, however, and reflects only statistical associations between variables; further investigation is needed to determine whether these relationships are causal in nature and exactly how they operate. Moreover, ecosystem dynamics and resilience are complex, involving potentially many factors beyond those considered here, as well as indirect or multivariate effects (Dakos et al., 2024; May, 1997; Walker, 2020). Yet we also note that the factors considered here are in line with previous work and are considered the predominant global and local factors impacting rainforests worldwide (Boulton et al., 2022; Flores et al., 2024; Hirota et al., 2011; Loreau & de Mazancourt, 2013; Oliver et al., 2015a, 2015b; Verbesselt et al., 2016).

It is important to note that while early-warning signals derived from CSD provide an indication of resilience loss and increasing proximity to a possible tipping point, they cannot accurately predict when a critical transition might occur (Dakos et al., 2015; Forzieri et al., 2022). Therefore, these

early-warning signals may highlight increased risk of forest instability and vulnerability to hazards, but they lack the ability to predict the exact time and extent of the potential system change. As such, they may be a useful guide to prioritizing action in conservation initiatives within Borneo, such as the Heart of Borneo (Sloan et al., 2019). However, critical transitions may occur without the presence of CSD, particularly in cases where process or observation errors are substantial, or when the system rapidly approaches a critical transition (Biggs et al., 2009; Carpenter & Brock, 2010; Perretti & Munch, 2012). Conversely, CSD may also produce false alarms, not truly reflecting actual dynamic changes in the system, such as when mechanisms of random disturbances change (Dakos et al., 2015; Dakos, van Nes, et al., 2012). We acknowledge that although we substantially reduced the likelihood of our results falling under one of these errors by combining the two resilience indicators, AC(1) and variance, these risks may nonetheless persist in our findings. Integrating our results alongside more fine-grained biodiversity and ecosystem health monitoring, as well as with larger scale mechanistic models of rainforests, may help further overcome this uncertainty and produce a more detailed picture of Bornean rainforest health and resilience overall.

Our findings confirm that long-term resilience loss in rainforests is a pan-tropical issue, and that the trend appears to be shaped by spatial variations in both biotic and abiotic factors. These insights may inform scientific guidance for the conservation and management of rainforests, especially in terms of addressing climate change, managing human activities, and protecting biodiversity. Our results indicate that trends in vegetation resilience loss observed around the world, and in particular in the Amazon, extend to Borneo, but that regional variation in key global drivers (e.g., global warming) and local factors interplay to cause differences in the underlying mechanics, breakpoint, magnitude and consistency of Bornean rainforest resilience loss. Nevertheless, our expanded evidence of declining resilience towards a possible tipping point of mass forest dieback in Borneo further emphasises the need for regional and global rainforest conservation and management coupled with climate change mitigation.

Methods

Datasets and Preprocessing

We defined the geographical extent of Borneo (7°N to 4°S, 108°E to 119°E) by integrating shapefiles of Malaysia, Brunei, and Indonesia from the GADM database version 4.1 (https://gadm.org/data.html, accessed 17 November 2023). To identify the intact rainforest of Borneo as our study area, we applied filters to the International Geosphere-Biosphere Programme (IGBP) Moderate Resolution Imaging Spectroradiometer (MODIS) land cover dataset MCD12C1 v061 (Friedl & Sulla-Menashe, 2022). We selected grid cells where evergreen broadleaf forest cover was ≥ 80% in 2001 and excluded any cells containing human land use (built-up, croplands, or vegetation mosaics > 0%; Boulton et al., 2022).

To evaluate the resilience of intact Bornean rainforest, we used VOD data from the Vegetation Optical Depth Climate Archive (VODCA; Moesinger et al., 2020). Compared to optical remote sensing vegetation products, such as Normalized Difference Vegetation Index (NDVI), passive microwave-derived VOD has the advantages of high sensitivity to high biomass levels, and the capability to perform under cloud cover, making it particularly suitable for tropical forest analysis (Liu et al., 2011, 2015; van Marle et al., 2016). VOD products with shorter wavelengths are more sensitive to leaf moisture content and better reflect changes in vegetation resilience, but are less influenced by stem biomass and soil moisture (Frappart et al., 2020; Konings et al., 2019; Moesinger et al., 2020). The Ku-band of VODCA was selected because it is the shortest wavelength band of the dataset, while providing the longest time span of short wavelength products by combining multiple sensors (Frappart et al., 2020; Moesinger et al., 2020).

To explore factors that may affect resilience change, we considered three perspectives: climate, human activity, and biodiversity. For climate, we focused on precipitation and temperature, sourced from the monthly average precipitation data of the Climate Hazards Center InfraRed Precipitation with Station data (CHIRPS) v2.0 dataset (Funk et al., 2015) and the fifth generation of European ReAnalysis (ERA5) Land monthly average 2 m air temperature dataset (Muñoz Sabater, 2019), respectively. Impacts of human activity were assessed using human footprint data from the database described by Mu et al. (2022). To avoid potential interference between plant diversity and VOD-derived resilience, we focused on animal biodiversity when exploring the relationship between

biodiversity and resilience. Specifically, we utilized animal species richness data from the International Union for Conservation of Nature (IUCN) Red List version 2022-2 (IUCN, 2022), including four taxa groups (amphibians, birds, mammals, and reptiles).

Preliminary exploration of the data highlighted significant fluctuations in the first three years of VODCA data, which were also reported by Boulton et al. (2022). Therefore, we also restricted our analysis to 1991-2016. The land cover dataset was only available from 2001 and was used up to 2016 to match the study period. We adopted a 0.25° × 0.25° spatial resolution, matching that of the VOD data (the coarsest dataset we examined) and unified the data under the WGS 1984 geographic reference system. We then aggregated data with different collection frequencies to the required analysis scale and cropped all data into the study area using the package terra (Hijmans, 2023) from R (v. 4.4.1; R Core Team, 2024).

Generation of Resilience Indicators

We used the VOD time series to estimate the resilience indicators, AC(1) and variance. We first applied the Seasonal and Trend decomposition using Loess (STL) to remove the long-term trends and seasonal fluctuations from the VOD data (Cleveland et al., 1990), in order to obtain a stationary time series of fluctuations to the system state, mostly caused by small perturbations (Dakos, Carpenter, et al., 2012; Tsay & Tiao, 1984). We used the stl() function in R (v.4.4.1; R Core Team, 2024) to decompose the time series in each grid cell (using the 'periodic' option for seasonal windows), retaining the residuals for subsequent analysis (Boulton et al, 2022).

AC(1) was calculated by fitting an order 1 autoregressive model (Dakos et al., 2008):

$$x_{t+1} = \alpha_1 x_t + \varepsilon_t$$

fit using ordinary least squares (OLS) with Gaussian random error ε_t. This formula does not include an intercept because the model's analysis was performed on detrended residuals with a mean of zero (Dakos et al., 2008).

We calculated resilience indicators over a 5-year (60-month) monthly sliding window, creating a new time series from July 1993 to July 2014. Importantly, to calculate overall resilience indicators for the entirety of Borneo, we first spatially averaged the VOD time series and then computed

resilience indicators on the mean VOD time series. This order of operations has proven more effective in reducing bias, especially that which arises from mixing sensors, compared to averaging resilience indicators computed for each grid cell (Smith et al., 2023). To explore the spatial variation of resilience loss across Borneo, we calculated the resilience indicators for each grid cell following the same sliding window approach.

Previous work has shown that AC(1) is a more robust indicator when analysing resilience (Boulton et al., 2013; Dakos, van Nes, et al., 2012), especially as variance is more susceptible to noise in ecosystem data and changes in environmental perturbations, hence we focus primarily on AC(1) in our analyses. However, Smith et al. (2023) recently highlighted that combining data from different sensors, such as VODCA, may also contribute to a rise in autocorrelation. They also point out that combined sensor data may bias AC(1) and variance toward negative correlation with one another, whereas actual resilience loss should yield increases in both AC(1) and variance (Boulton et al., 2022; Smith et al., 2023). Therefore, we mainly employ variance as a supplementary metric to validate that the increases in AC(1) are likely due to resilience loss. To further examine the potential influence of satellite sensor transitions on the VODCA products, we incorporated the timing of these shifts into the mean AC(1) series and compared these with the breakpoint (Supplementary Fig. 1).

Metrics of Resilience

A Bayesian changepoint detection algorithm was used to reveal when trends in resilience changed, employing the package mcp (Lindeløv, 2020) from R (v.4.4.1; R Core Team, 2024). Though the Kendall τ non-parametric rank correlation coefficient is used as a general indicator for evaluating trends in other parts of the study, in the analysis of trends in resilience it was specifically used to assess the consistency of changes in the AC(1) time series for the full study period and after the corresponding breakpoint. Kendall τ returns values of 1 for a consistently increasing series, -1 for a consistently decreasing series, and 0 when there is no overall trend. Additionally, we calculated the slope of linear regressions fit to the full study period and the periods before and after the breakpoint, to reveal the overall rate and magnitude of changes in AC(1). To specifically examine the magnitude of change in the rate of resilience loss post-breakpoint, we also calculated Δslope, the

difference in slope of linear regressions fit pre- and post-breakpoint. Positive Δslope values indicate an accelerating loss of resilience (or decreased rate of resilience gain), while negative values indicate a slowing down of resilience loss (or accelerating resilience gain).

The *p*-value directly derived from the Kendall τ coefficient may be inaccurate due to its sensitivity to the autocorrelation characteristic inherent in time series data. Therefore, following prior work, we employed a phase randomization procedure to generate surrogate data to determine the significance of Kendall τ (Boers, 2018; Boulton et al., 2022; Dakos et al., 2008). Specifically, we performed a Fourier transform on the AC(1) time series, randomly permuted the phases, and then applied an inverse Fourier transform, thereby maintaining the autocorrelation and variance in the surrogate series (Boulton et al., 2022; Theiler et al., 1992). We performed this 100,000 times to create a null model for assessing the significance of Kendall τ. The *p*-value was determined by calculating the proportion of surrogates that exhibit a higher Kendall τ value than that observed in the actual series.

Factors Correlated with Resilience Change

We used four factors - mean annual precipitation, mean annual temperature, human footprint and species richness - to explore potential relationships between vegetation resilience and climate, human activity, and biodiversity. We treated each factor as a constant, to focus on changes in resilience and standardize the analysis of all factors. Factors with time-series data, such as precipitation and temperature, were thus averaged over the study period for subsequent analysis, allowing us to focus solely on the spatial patterns in the factors and resilience change. We also calculated Spearman correlations to assess spatial correlations between the factors, given several factors had non-normal distributions and could have nonlinear relationships.

We explored the impact of various factors on resilience by ranking the values of each factor and applying a sliding band, where a fixed number of grid cells of 100 were used across the data range, shifting the band by one grid cell at each step. These bands were then used to spatially subset grid cells that fell within the range of factors' values for each band. For each subset, we calculated the AC(1) time series from the VOD time series of the selected grid cells following the same approach we used for the entirety of Borneo and estimated the three metrics of resilience change, Finally, we used a linear model to assess the correlation between each factor and the resilience metrics.

Robustness Tests

To test the robustness of the results, we varied the evergreen broadleaf forest cover thresholds used to define the study area. Specifically, we estimated the AC(1) trend when the forest cover threshold is set to ≥ 60% and ≥ 90% (Supplementary Figs. 2, 3). We also tested the robustness of the sliding window length used to calculate AC(1) by trying windows of 30, 90, and 120 months in length (Supplementary Fig. 4). For exploration of the relationship between factors and resilience loss pattern, we also use sliding bands of 50 grid cells (Supplementary Figs. 10, 11).

Figures

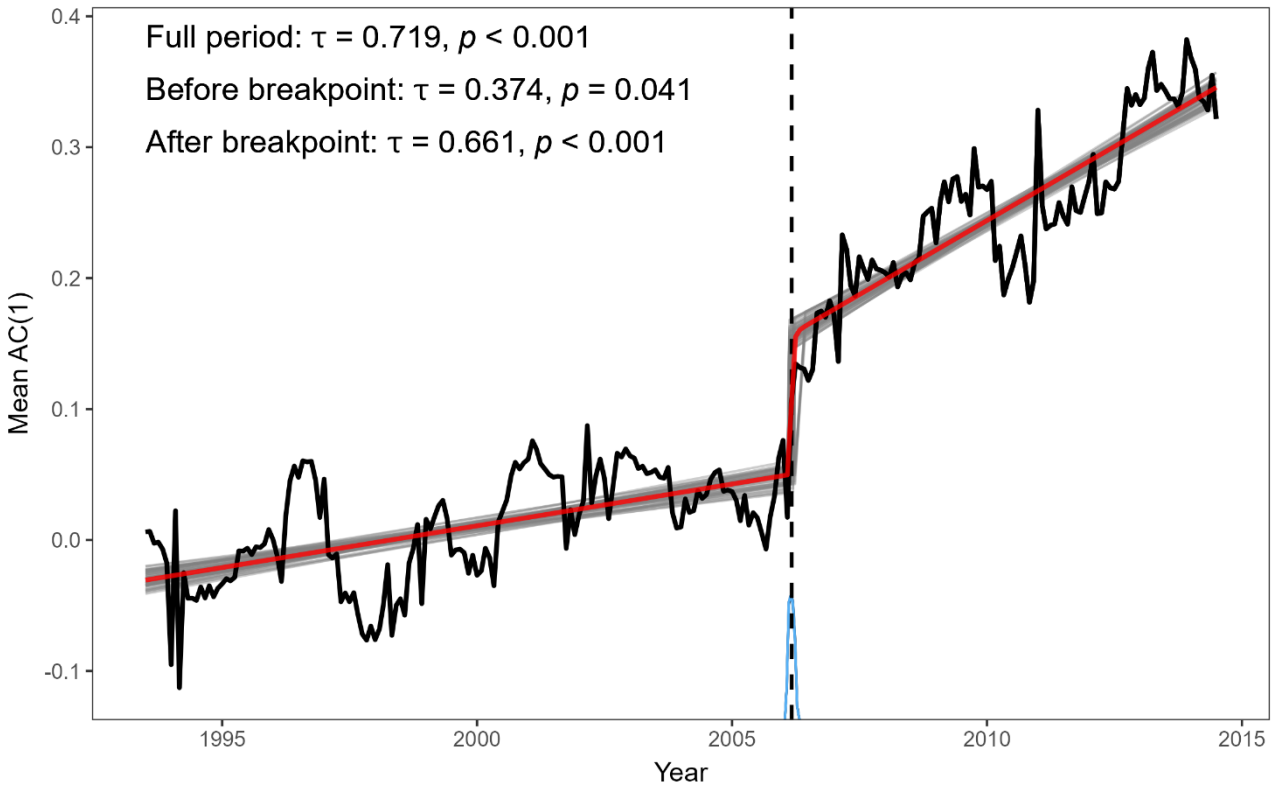

Fig.1 Overall resilience changes in Bornean rainforest. Mean VOD AC(1) time series of the study area from July 1993 to July 2014, calculated on 5-year monthly sliding windows and plotted at the midpoint of each window. The red line represents the posterior mean of the segmented linear fit to the AC(1) time series, with the grey lines showing posterior-draw fits (n = 50 for display, n = 50,000 for analysis). The vertical dashed line indicates the posterior mean breakpoint, with the blue curve below showing its posterior distribution. The trend of AC(1) time series for the full record, pre-breakpoint, and post-breakpoint periods are calculated using Kendall τ, shown in the upper left with associated p-values.

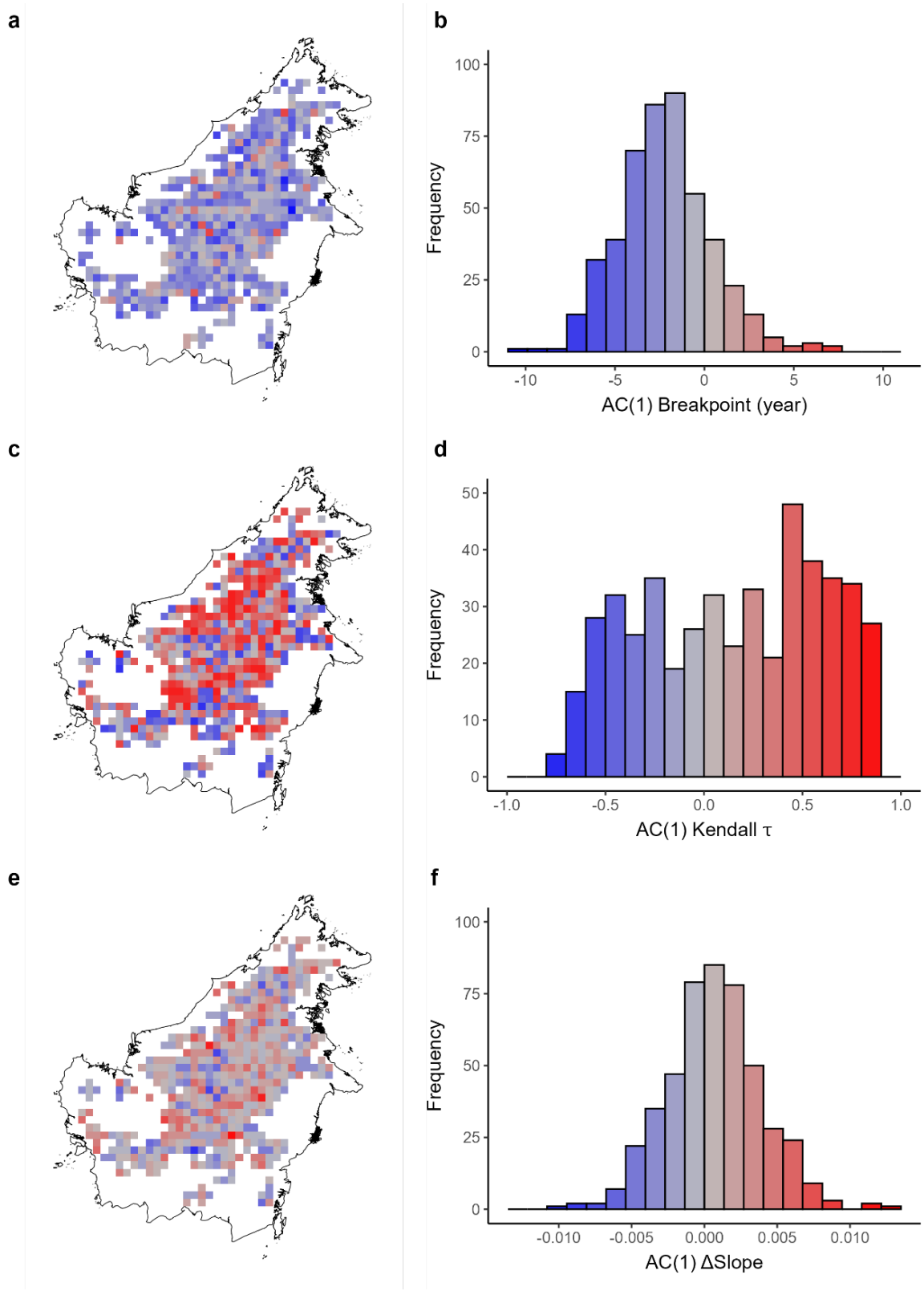

Fig. 2 Spatial patterns of changes in Bornean rainforest. a, Spatial distribution of the breakpoint calculated from AC(1) time series of each grid cell, with the same colour coding as in **b**. **b,** Histogram of the differences between the breakpoint of each grid cell compared to the breakpoint of entire study area (March 2006). **c-f,** Spatial distribution of post-breakpoint AC(1) Kendall τ values **(c)** and changes in the slope of linear fitted AC(1) time series before and after the breakpoint **(e)**, with corresponding histograms of their values shown using the same colour coding in **d** and **f**, respectively.

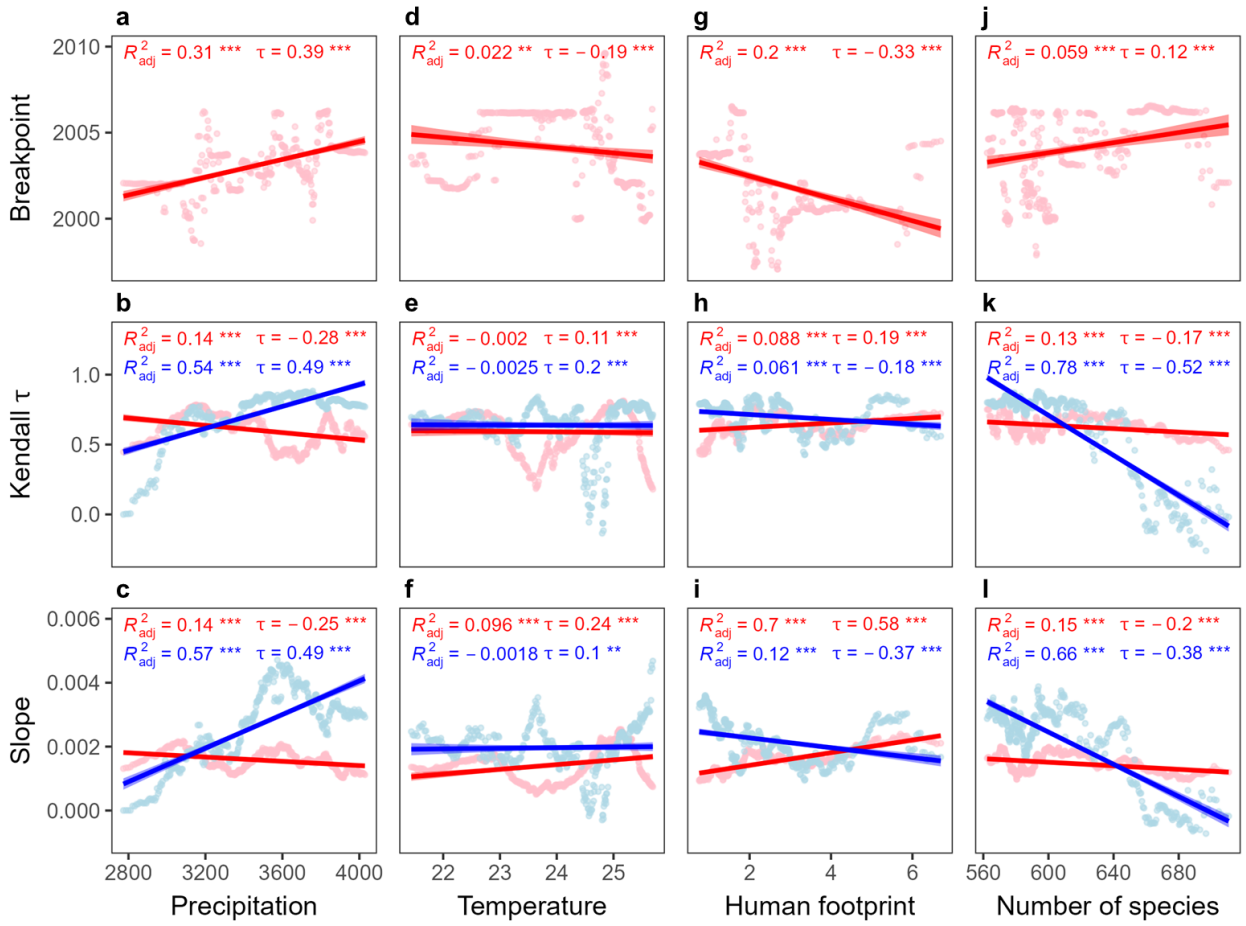

Fig. 3 Relationship between potential influencing factors and resilience (sliding band size = 100 cells). a-c, Correlation between precipitation and the following resilience metrics calculated on sliding bands of grid cells along a precipitation gradient (Methods): breakpoint **(a)**, Kendall τ (red: full study period; blue: post-breakpoint) **(b)**. and linear regression slope (red: full study period; blue: post-breakpoint) **(c)**. We use the raw slope values rather than Δslope in order to allow comparison between the full study period and post-breakpoint period. The correlations between the resilience metrics and potential influencing factors are calculated using Kendall τ and linear models. The Kendall τ and adjusted-R^2 values are reported in each panel with their p-values denoted by stars (***: $p \leq 0.001$, **: $p \leq 0.01$, *: $p \leq 0.05$). **d-l**, The same as **a-c**, but for temperature, human footprint and species richness, respectively. In each panel, the values are plotted at the midpoint of each band.

Data Availability

The shapefiles for the countries are available from https://gadm.org/data.html. The VOD dataset is available from https://zenodo.org/record/2575599#.YHRE6RRKj7E. The MODIS Land Cover dataset is available from https://lpdaac.usgs.gov/products/mcd12c1v061. The CHIRPS precipitation dataset is available from https://data.chc.ucsb.edu/products/CHIRPS-2.0/global_monthly/tifs. The ERA5-Land temperature dataset is available from https://cds.climate.copernicus.eu/cdsapp#!/dataset/reanalysis-era5-land-monthly-means?tab=overview. The human footprint dataset is available from https://figshare.com/articles/figure/An_annual_global_terrestrial_Human_Footprint_dataset_from_2000_to_2018/16571064. The IUCN Red List Species Richness dataset is available from https://www.iucnredlist.org/resources/other-spatial-downloads.

Acknowledgements

We thank Chris A. Boulton for helpful discussions as well as members of the Ewers group for feedback on earlier drafts, including David Orme, Vivienne P. Groner, Jacob Cook, Hollie Folkard-Tapp and Olivia Daniel. N.P.L.P. was supported by the Natural Environment Research Council (grant number NE/S007415/1) via the Science and Solutions for a Changing Planet DTP.

Author contributions

The study was conceptualised by all authors. Data processing and statistical analyses were conducted by S.C. The project was supervised by R.M.E and N.P.L.P. The original draft was written by S.C. and N.P.L.P. All authors contributed to revising and editing the final manuscript.

Competing interests

The authors declare no competing interests.

References

Achard, F., Eva, H. D., Stibig, H.-J., Mayaux, P., Gallego, J., Richards, T., & Malingreau, J.-P. (2002). Determination of deforestation rates of the world's humid tropical forests. *Science*, *297*(5583), 999–1002. https://doi.org/10.1126/science.1070656

Aguirre-Gutiérrez, J., Berenguer, E., Oliveras Menor, I., Bauman, D., Corral-Rivas, J. J., Nava-Miranda, M. G., Both, S., Ndong, J. E., Ondo, F. E., Bengone, N. N., Mihinhou, V., Dalling, J. W., Heineman, K., Figueiredo, A., González-M, R., Norden, N., Hurtado-M, A. B., González, D., Salgado-Negret, B., … Malhi, Y. (2022). Functional susceptibility of tropical forests to climate change. *Nature Ecology & Evolution*, *6*(7), 878–889. https://doi.org/10.1038/s41559-022-01747-6

Allen, C. D., Macalady, A. K., Chenchouni, H., Bachelet, D., McDowell, N., Vennetier, M., Kitzberger, T., Rigling, A., Breshears, D. D., Hogg, E. H. (Ted), Gonzalez, P., Fensham, R., Zhang, Z., Castro, J., Demidova, N., Lim, J.-H., Allard, G., Running, S. W., Semerci, A., & Cobb, N. (2010). A global overview of drought and heat-induced tree mortality reveals emerging climate change risks for forests. *Adaptation of Forests and Forest Management to Changing Climate*, *259*(4), 660–684. https://doi.org/10.1016/j.foreco.2009.09.001

Biggs, R., Carpenter, S. R., & Brock, W. A. (2009). Turning back from the brink: Detecting an impending regime shift in time to avert it. *Proceedings of the National Academy of Sciences*, *106*(3), 826–831. https://doi.org/10.1073/pnas.0811729106

Boers, N. (2018). Early-warning signals for Dansgaard-Oeschger events in a high-resolution ice core record. *Nature Communications*, *9*(1), 2556. https://doi.org/10.1038/s41467-018-04881-7

Boers, N. (2021). Observation-based early-warning signals for a collapse of the Atlantic Meridional Overturning Circulation. *Nature Climate Change*, *11*(8), 680–688. https://doi.org/10.1038/s41558-021-01097-4

Boers, N., & Rypdal, M. (2021). Critical slowing down suggests that the western Greenland Ice Sheet is close to a tipping point. *Proceedings of the National Academy of Sciences*, *118*(21), e2024192118. https://doi.org/10.1073/pnas.2024192118

Boulton, C. A., Booth, B. B. B., & Good, P. (2017). Exploring uncertainty of Amazon dieback in a perturbed parameter Earth system ensemble. *Global Change Biology*, *23*(12), 5032–5044. https://doi.org/10.1111/gcb.13733

Boulton, C. A., Good, P., & Lenton, T. M. (2013). Early warning signals of simulated Amazon rainforest

dieback. *Theoretical Ecology*, *6*(3), 373–384. https://doi.org/10.1007/s12080-013-0191-7

Boulton, C. A., Lenton, T. M., & Boers, N. (2022). Pronounced loss of Amazon rainforest resilience since the early 2000s. *Nature Climate Change*, *12*(3), 271–278. https://doi.org/10.1038/s41558-022-01287-8

Carpenter, S. R., & Brock, W. A. (2010). Early warnings of regime shifts in spatial dynamics using the discrete Fourier transform. *Ecosphere*, *1*(5), art10. https://doi.org/10.1890/ES10-00016.1

Carpenter, S. R., Cole, J. J., Pace, M. L., Batt, R., Brock, W. A., Cline, T., Coloso, J., Hodgson, J. R., Kitchell, J. F., Seekell, D. A., Smith, L., & Weidel, B. (2011). Early warnings of regime shifts: A whole-ecosystem experiment. *Science*, *332*(6033), 1079–1082. https://doi.org/10.1126/science.1203672

Clements, C. F., & Ozgul, A. (2018). Indicators of transitions in biological systems. *Ecology Letters*, *21*(6), 905–919. https://doi.org/10.1111/ele.12948

Cleveland, R. B., Cleveland, W. S., McRae, J. E., & Terpenning, I. (1990). STL: A seasonal-trend decomposition. *Journal of Official Statistics*, *6*(1), 3–73.

Coux, C., Rader, R., Bartomeus, I., & Tylianakis, J. M. (2016). Linking species functional roles to their network roles. *Ecology Letters*, *19*(7), 762–770. https://doi.org/10.1111/ele.12612

Da Silveira Lobo Sternberg, L. (2001). Savanna–forest hysteresis in the tropics. *Global Ecology and Biogeography*, *10*(4), 369–378. https://doi.org/10.1046/j.1466-822X.2001.00243.x

Dai, L., Vorselen, D., Korolev, K. S., & Gore, J. (2012). Generic indicators for loss of resilience before a tipping point leading to population collapse. *Science*, *336*(6085), 1175–1177. https://doi.org/10.1126/science.1219805

Dakos, V., Boulton, C. A., Buxton, J. E., Abrams, J. F., Arellano-Nava, B., Armstrong McKay, D. I., Bathiany, S., Blaschke, L., Boers, N., Dylewsky, D., López-Martínez, C., Parry, I., Ritchie, P., van der Bolt, B., van der Laan, L., Weinans, E., & Kéfi, S. (2024). Tipping point detection and early warnings in climate, ecological, and human systems. *Earth System Dynamics*, *15*(4), 1117–1135. https://doi.org/10.5194/esd-15-1117-2024

Dakos, V., Carpenter, S. R., van Nes, E. H., & Scheffer, M. (2015). Resilience indicators: Prospects and limitations for early warnings of regime shifts. *Philosophical Transactions of the Royal Society B: Biological Sciences*, *370*(1659), 20130263. https://doi.org/10.1098/rstb.2013.0263

Dakos, V., & Kéfi, S. (2022). Ecological resilience: What to measure and how. *Environmental Research Letters*, *17*(4), 043003. https://doi.org/10.1088/1748-9326/ac5767

Dakos, V., Scheffer, M., van Nes, E. H., Brovkin, V., Petoukhov, V., & Held, H. (2008). Slowing down as an early warning signal for abrupt climate change. *Proceedings of the National Academy of Sciences*, *105*(38), 14308–14312. https://doi.org/10.1073/pnas.0802430105

Dakos, V., van Nes, E. H., D'Odorico, P., & Scheffer, M. (2012). Robustness of variance and autocorrelation as indicators of critical slowing down. *Ecology*, *93*(2), 264–271. https://doi.org/10.1890/11-0889.1

Drake, J. M., & Griffen, B. D. (2010). Early warning signals of extinction in deteriorating environments. *Nature*, *467*(7314), 456–459. https://doi.org/10.1038/nature09389

Elmqvist, T., Folke, C., Nyström, M., Peterson, G., Bengtsson, J., Walker, B., & Norberg, J. (2003). Response diversity, ecosystem change, and resilience. *Frontiers in Ecology and the Environment*, *1*(9), 488–494. https://doi.org/10.1890/1540-9295(2003)001[0488:RDECAR]2.0.CO;2

Ferraz, S. F. B., Ferraz, K. M. P. M. B., Cassiano, C. C., Brancalion, P. H. S., da Luz, D. T. A., Azevedo, T. N., Tambosi, L. R., & Metzger, J. P. (2014). How good are tropical forest patches for ecosystem services provisioning? *Landscape Ecology*, *29*(2), 187–200. https://doi.org/10.1007/s10980-014-9988-z

Flores, B. M., Montoya, E., Sakschewski, B., Nascimento, N., Staal, A., Betts, R. A., Levis, C., Lapola, D. M., Esquível-Muelbert, A., Jakovac, C., Nobre, C. A., Oliveira, R. S., Borma, L. S., Nian, D., Boers, N., Hecht, S. B., ter Steege, H., Arieira, J., Lucas, I. L., … Hirota, M. (2024). Critical transitions in the Amazon forest system. *Nature*, *626*(7999), 555–564. https://doi.org/10.1038/s41586-023-06970-0

Forzieri, G., Dakos, V., McDowell, N. G., Ramdane, A., & Cescatti, A. (2022). Emerging signals of declining forest resilience under climate change. *Nature*, *608*(7923), 534–539. https://doi.org/10.1038/s41586-022-04959-9

Frappart, F., Wigneron, J.-P., Li, X., Liu, X., Al-Yaari, A., Fan, L., Wang, M., Moisy, C., Le Masson, E., Aoulad Lafkih, Z., Vallé, C., Ygorra, B., & Baghdadi, N. (2020). Global monitoring of the vegetation dynamics from the vegetation optical depth (VOD): A review. *Remote Sensing*, *12*(18). https://doi.org/10.3390/rs12182915

Friedl, M., & Sulla-Menashe, D. (2022). *MODIS/Terra+Aqua Land Cover Type Yearly L3 Global 0.05Deg CMG V061* [Dataset]. NASA EOSDIS Land Processes Distributed Active Archive Center. https://doi.org/10.5067/MODIS/MCD12C1.061

Funk, C., Peterson, P., Landsfeld, M., Pedreros, D., Verdin, J., Shukla, S., Husak, G., Rowland, J., Harrison,

L., Hoell, A., & Michaelsen, J. (2015). The climate hazards infrared precipitation with stations—A new environmental record for monitoring extremes. *Scientific Data*, *2*(1), 150066. https://doi.org/10.1038/sdata.2015.66

Gallagher, R. V., Hughes, L., & Leishman, M. R. (2013). Species loss and gain in communities under future climate change: Consequences for functional diversity. *Ecography*, *36*(5), 531–540. https://doi.org/10.1111/j.1600-0587.2012.07514.x

Gardner, T. A., Barlow, J., Chazdon, R., Ewers, R. M., Harvey, C. A., Peres, C. A., & Sodhi, N. S. (2009). Prospects for tropical forest biodiversity in a human-modified world. *Ecology Letters*, *12*(6), 561–582. https://doi.org/10.1111/j.1461-0248.2009.01294.x

Hansen, M. C., Potapov, P. V., Moore, R., Hancher, M., Turubanova, S. A., Tyukavina, A., Thau, D., Stehman, S. V., Goetz, S. J., Loveland, T. R., Kommareddy, A., Egorov, A., Chini, L., Justice, C. O., & Townshend, J. R. G. (2013). High-resolution global maps of 21st-century forest cover change. *Science*, *342*(6160), 850–853. https://doi.org/10.1126/science.1244693

Hastings, A. (2010). Timescales, dynamics, and ecological understanding. *Ecology*, *91*(12), 3471–3480. https://doi.org/10.1890/10-0776.1

Hijmans, R. J. (2024). terra: Spatial data analysis (version 1.7-78). https://CRAN.R-project.org/package=terra

Hirota, M., Holmgren, M., Van Nes, E. H., & Scheffer, M. (2011). Global resilience of tropical forest and savanna to critical transitions. *Science*, *334*(6053), 232–235. https://doi.org/10.1126/science.1210657

Holling, C. S. (1973). Resilience and stability of ecological systems. *Annual Review of Ecology, Evolution, and Systematics, 4*(4), 1-23. https://doi.org/10.1146/annurev.es.04.110173.000245

Holling, C. S. (1996). Engineering resilience versus ecological resilience. *Engineering within Ecological Constraints*, *31*(1996), 32.

Houghton, R. A., Byers, B., & Nassikas, A. A. (2015). A role for tropical forests in stabilizing atmospheric CO2. *Nature Climate Change*, *5*(12), 1022–1023. https://doi.org/10.1038/nclimate2869

Ibáñez, I., Acharya, K., Juno, E., Karounos, C., Lee, B. R., McCollum, C., Schaffer-Morrison, S., & Tourville, J. (2019). Forest resilience under global environmental change: Do we have the information we need? A systematic review. *PLOS ONE*, *14*(9), e0222207. https://doi.org/10.1371/journal.pone.0222207

IUCN. (2022). *The IUCN red list of threatened species* (Version 2022-2) [Dataset].

https://www.iucnredlist.org

Ives, A. R. (1995). Measuring resilience in stochastic systems. *Ecological Monographs*, *65*(2), 217–233. https://doi.org/10.2307/2937138

Jones, C., Lowe, J., Liddicoat, S., & Betts, R. (2009). Committed terrestrial ecosystem changes due to climate change. *Nature Geoscience*, *2*(7), 484–487. https://doi.org/10.1038/ngeo555

Kéfi, S., Domínguez-García, V., Donohue, I., Fontaine, C., Thébault, E., & Dakos, V. (2019). Advancing our understanding of ecological stability. *Ecology Letters*, *22*(9), 1349–1356. https://doi.org/10.1111/ele.13340

Konings, A. G., Rao, K., & Steele-Dunne, S. C. (2019). Macro to micro: Microwave remote sensing of plant water content for physiology and ecology. *New Phytologist*, *223*(3), 1166–1172. https://doi.org/10.1111/nph.15808

Lenton, T. M., Abrams, J. F., Bartsch, A., Bathiany, S., Boulton, C. A., Buxton, J. E., Conversi, A., Cunliffe, A. M., Hebden, S., Lavergne, T., Poulter, B., Shepherd, A., Smith, T., Swingedouw, D., Winkelmann, R., & Boers, N. (2024). Remotely sensing potential climate change tipping points across scales. *Nature Communications*, *15*(1), 343. https://doi.org/10.1038/s41467-023-44609-w

Lenton, T. M., Buxton, J. E., Armstrong McKay, D. I., Abrams, J. F., Boulton, C. A., Lees, K., Powell, T. W. R., Boers, N., Cunliffe, A. M., & Dakos, V. (2022). A resilience sensing system for the biosphere. *Philosophical Transactions of the Royal Society B: Biological Sciences*, *377*(1857), 20210383. https://doi.org/10.1098/rstb.2021.0383

Lenton, T. M., Held, H., Kriegler, E., Hall, J. W., Lucht, W., Rahmstorf, S., & Schellnhuber, H. J. (2008). Tipping elements in the Earth's climate system. *Proceedings of the National Academy of Sciences*, *105*(6), 1786–1793. https://doi.org/10.1073/pnas.0705414105

Levin, S. A. (1992). The problem of pattern and scale in ecology: The Robert H. MacArthur award lecture. *Ecology*, *73*(6), 1943–1967. https://doi.org/10.2307/1941447

Lindeløv, J. K. (2020). mcp: An R package for regression with multiple change points. *OSF Preprints*. https://doi.org/10.31219/osf.io/fzqxv

Liu, Y. Y., de Jeu, R. A. M., McCabe, M. F., Evans, J. P., & van Dijk, A. I. J. M. (2011). Global long-term passive microwave satellite-based retrievals of vegetation optical depth. *Geophysical Research Letters*, *38*(18). https://doi.org/10.1029/2011GL048684

Liu, Y. Y., van Dijk, A. I. J. M., de Jeu, R. A. M., Canadell, J. G., McCabe, M. F., Evans, J. P., & Wang, G.

(2015). Recent reversal in loss of global terrestrial biomass. *Nature Climate Change*, *5*(5), 470–474. https://doi.org/10.1038/nclimate2581

Loreau, M., & de Mazancourt, C. (2013). Biodiversity and ecosystem stability: A synthesis of underlying mechanisms. *Ecology Letters*, *16*(s1), 106–115. https://doi.org/10.1111/ele.12073

Malhi, Y., Roberts, J. T., Betts, R. A., Killeen, T. J., Li, W., & Nobre, C. A. (2008). Climate change, deforestation, and the fate of the Amazon. *Science*, *319*(5860), 169–172. https://doi.org/10.1126/science.1146961

May, R. M. (1972). Will a large complex system be stable? *Nature*, *238*(5364), 413–414. https://doi.org/10.1038/238413a0

May, R. M. (1987). Chaos and the dynamics of biological populations. *Proceedings of the Royal Society of London. A. Mathematical and Physical Sciences*, *413*(1844), 27–44. https://doi.org/10.1098/rspa.1987.0098

Moesinger, L., Dorigo, W., de Jeu, R., van der Schalie, R., Scanlon, T., Teubner, I., & Forkel, M. (2020). The global long-term microwave Vegetation Optical Depth Climate Archive (VODCA). *Earth System Science Data*, *12*(1), 177–196. https://doi.org/10.5194/essd-12-177-2020

Morris, R. J. (2010). Anthropogenic impacts on tropical forest biodiversity: A network structure and ecosystem functioning perspective. *Philosophical Transactions of the Royal Society B: Biological Sciences*, *365*(1558), 3709–3718. https://doi.org/10.1098/rstb.2010.0273

Mouillot, D., Graham, N. A. J., Villéger, S., Mason, N. W. H., & Bellwood, D. R. (2013). A functional approach reveals community responses to disturbances. *Trends in Ecology & Evolution*, *28*(3), 167–177. https://doi.org/10.1016/j.tree.2012.10.004

Mu, H., Li, X., Wen, Y., Huang, J., Du, P., Su, W., Miao, S., & Geng, M. (2022). A global record of annual terrestrial Human Footprint dataset from 2000 to 2018. *Scientific Data*, *9*(1), 176. https://doi.org/10.1038/s41597-022-01284-8

Muñoz Sabater, J. (2019). *ERA5-Land monthly averaged data from 1950 to present* [Dataset]. Copernicus Climate Change Service Climate Data Store. https://doi.org/10.24381/cds.68d2bb30

Nepstad, D., McGrath, D., Stickler, C., Alencar, A., Azevedo, A., Swette, B., Bezerra, T., DiGiano, M., Shimada, J., Seroa da Motta, R., Armijo, E., Castello, L., Brando, P., Hansen, M. C., McGrath-Horn, M., Carvalho, O., & Hess, L. (2014). Slowing Amazon deforestation through public policy and interventions in beef and soy supply chains. *Science*, *344*(6188), 1118–1123.

https://doi.org/10.1126/science.1248525

Neuschulz, E. L., Mueller, T., Schleuning, M., & Böhning-Gaese, K. (2016). Pollination and seed dispersal are the most threatened processes of plant regeneration. *Scientific Reports*, *6*(1), 29839. https://doi.org/10.1038/srep29839

Oliver, T. H., Heard, M. S., Isaac, N. J. B., Roy, D. B., Procter, D., Eigenbrod, F., Freckleton, R., Hector, A., Orme, C. D. L., Petchey, O. L., Proença, V., Raffaelli, D., Suttle, K. B., Mace, G. M., Martín-López, B., Woodcock, B. A., & Bullock, J. M. (2015a). Biodiversity and resilience of ecosystem functions. *Trends in Ecology & Evolution*, *30*(11), 673–684. https://doi.org/10.1016/j.tree.2015.08.009

Oliver, T. H., Isaac, N. J. B., August, T. A., Woodcock, B. A., Roy, D. B., & Bullock, J. M. (2015b). Declining resilience of ecosystem functions under biodiversity loss. *Nature Communications*, *6*(1), 10122. https://doi.org/10.1038/ncomms10122

Pan, Y., Birdsey, R. A., Fang, J., Houghton, R., Kauppi, P. E., Kurz, W. A., Phillips, O. L., Shvidenko, A., Lewis, S. L., Canadell, J. G., Ciais, P., Jackson, R. B., Pacala, S. W., McGuire, A. D., Piao, S., Rautiainen, A., Sitch, S., & Hayes, D. (2011). A large and persistent carbon sink in the world's forests. *Science*, *333*(6045), 988–993. https://doi.org/10.1126/science.1201609

Perretti, C. T., & Munch, S. B. (2012). Regime shift indicators fail under noise levels commonly observed in ecological systems. *Ecological Applications*, *22*(6), 1772–1779. https://doi.org/10.1890/11-0161.1

Petraitis, P. (2013). *Multiple stable states in natural ecosystems*. Oxford University Press. https://doi.org/10.1093/acprof:osobl/9780199569342.001.0001

Pimm, S. L. (1984). The complexity and stability of ecosystems. *Nature*, *307*(5949), 321–326. https://doi.org/10.1038/307321a0

R Core Team. (2024). R: A language and environment for statistical computing. R Foundation for Statistical Computing. https://www.R-project.org/

Reyer, C. P., Brouwers, N., Rammig, A., Brook, B. W., Epila, J., Grant, R. F., Holmgren, M., Langerwisch, F., Leuzinger, S., & Lucht, W. (2015). Forest resilience and tipping points at different spatio-temporal scales: Approaches and challenges. *Journal of Ecology*, *103*(1), 5–15. https://doi.org/10.1111/1365-2745.12337

Scheffer, M., Barrett, S., Carpenter, S. R., Folke, C., Green, A. J., Holmgren, M., Hughes, T. P., Kosten, S., van de Leemput, I. A., Nepstad, D. C., van Nes, E. H., Peeters, E. T. H. M., & Walker, B. (2015). Creating a safe operating space for iconic ecosystems. *Science*, *347*(6228), 1317–1319.

https://doi.org/10.1126/science.aaa3769

Scheffer, M., Bascompte, J., Brock, W. A., Brovkin, V., Carpenter, S. R., Dakos, V., Held, H., van Nes, E. H., Rietkerk, M., & Sugihara, G. (2009). Early-warning signals for critical transitions. *Nature*, *461*(7260), 53–59. https://doi.org/10.1038/nature08227

Scheffer, M., Carpenter, S., Foley, J. A., Folke, C., & Walker, B. (2001). Catastrophic shifts in ecosystems. *Nature*, *413*(6856), 591–596. https://doi.org/10.1038/35098000

Schröder, A., Persson, L., & De Roos, A. M. (2005). Direct experimental evidence for alternative stable states: A review. *Oikos*, *110*(1), 3–19. https://doi.org/10.1111/j.0030-1299.2005.13962.x

Shimamoto, C. Y., Padial, A. A., da Rosa, C. M., & Marques, M. C. M. (2018). Restoration of ecosystem services in tropical forests: A global meta-analysis. *PLOS ONE*, *13*(12), e0208523. https://doi.org/10.1371/journal.pone.0208523

Sloan, S., Campbell, M. J., Alamgir, M., Lechner, A. M., Engert, J., & Laurance, W. F. (2019). Trans-national conservation and infrastructure development in the Heart of Borneo. *PLOS ONE*, *14*(9), e0221947. https://doi.org/10.1371/journal.pone.0221947

Smith, T., Traxl, D., & Boers, N. (2022). Empirical evidence for recent global shifts in vegetation resilience. *Nature Climate Change*, *12*(5), 477–484. https://doi.org/10.1038/s41558-022-01352-2

Smith, T., Zotta, R.-M., Boulton, C. A., Lenton, T. M., Dorigo, W., & Boers, N. (2023). Reliability of resilience estimation based on multi-instrument time series. *Earth System Dynamics*, *14*(1), 173–183. https://doi.org/10.5194/esd-14-173-2023

Staal, A., Tuinenburg, O. A., Bosmans, J. H. C., Holmgren, M., van Nes, E. H., Scheffer, M., Zemp, D. C., & Dekker, S. C. (2018). Forest-rainfall cascades buffer against drought across the Amazon. *Nature Climate Change*, *8*(6), 539–543. https://doi.org/10.1038/s41558-018-0177-y

Steffen, W., Richardson, K., Rockström, J., Cornell, S. E., Fetzer, I., Bennett, E. M., Biggs, R., Carpenter, S. R., de Vries, W., de Wit, C. A., Folke, C., Gerten, D., Heinke, J., Mace, G. M., Persson, L. M., Ramanathan, V., Reyers, B., & Sörlin, S. (2015). Planetary boundaries: Guiding human development on a changing planet. *Science*, *347*(6223), 1259855. https://doi.org/10.1126/science.1259855

Strogatz, S. H. (1994). *Nonlinear dynamics and chaos: With applications to physics, biology, chemistry, and engineering*. Westview Press.

Theiler, J., Eubank, S., Longtin, A., Galdrikian, B., & Doyne Farmer, J. (1992). Testing for nonlinearity in time series: The method of surrogate data. *Physica D: Nonlinear Phenomena*, *58*(1), 77–94.

https://doi.org/10.1016/0167-2789(92)90102-S

Trumbore, S., Brando, P., & Hartmann, H. (2015). Forest health and global change. *Science*, *349*(6250), 814–818. https://doi.org/10.1126/science.aac6759

Tsay, R. S., & Tiao, G. C. (1984). Consistent estimates of autoregressive parameters and extended sample autocorrelation function for stationary and nonstationary ARMA models. *Journal of the American Statistical Association*, *79*(385), 84–96. https://doi.org/10.1080/01621459.1984.10477068

van Marle, M. J. E., van der Werf, G. R., de Jeu, R. A. M., & Liu, Y. Y. (2016). Annual South American forest loss estimates based on passive microwave remote sensing (1990–2010). *Biogeosciences*, *13*(2), 609–624. https://doi.org/10.5194/bg-13-609-2016

van Nes, E. H., & Scheffer, M. (2007). Slow recovery from perturbations as a generic Indicator of a nearby catastrophic shift. *The American Naturalist*, *169*(6), 738–747. https://doi.org/10.1086/516845

Van Passel, J., Bernardino, P. N., Lhermitte, S., Rius, B. F., Hirota, M., Conradi, T., de Keersmaecker, W., Van Meerbeek, K., & Somers, B. (2024). Critical slowing down of the Amazon forest after increased drought occurrence. *Proceedings of the National Academy of Sciences*, *121*(22), e2316924121. https://doi.org/10.1073/pnas.2316924121

Verbesselt, J., Umlauf, N., Hirota, M., Holmgren, M., Van Nes, E. H., Herold, M., Zeileis, A., & Scheffer, M. (2016). Remotely sensed resilience of tropical forests. *Nature Climate Change*, *6*(11), 1028–1031. https://doi.org/10.1038/nclimate3108

Walker, B. H. (2020). Resilience: What it is and is not. *Ecology and Society*, *25*(2). https://doi.org/10.5751/ES-11647-250211

Wang, R., Dearing, J. A., Langdon, P. G., Zhang, E., Yang, X., Dakos, V., & Scheffer, M. (2012). Flickering gives early warning signals of a critical transition to a eutrophic lake state. *Nature*, *492*(7429), 419–422. https://doi.org/10.1038/nature11655

Wissel, C. (1984). A universal law of the characteristic return time near thresholds. *Oecologia*, *65*, 101–107. https://doi.org/10.1007/BF00384470

Supplementary Figures

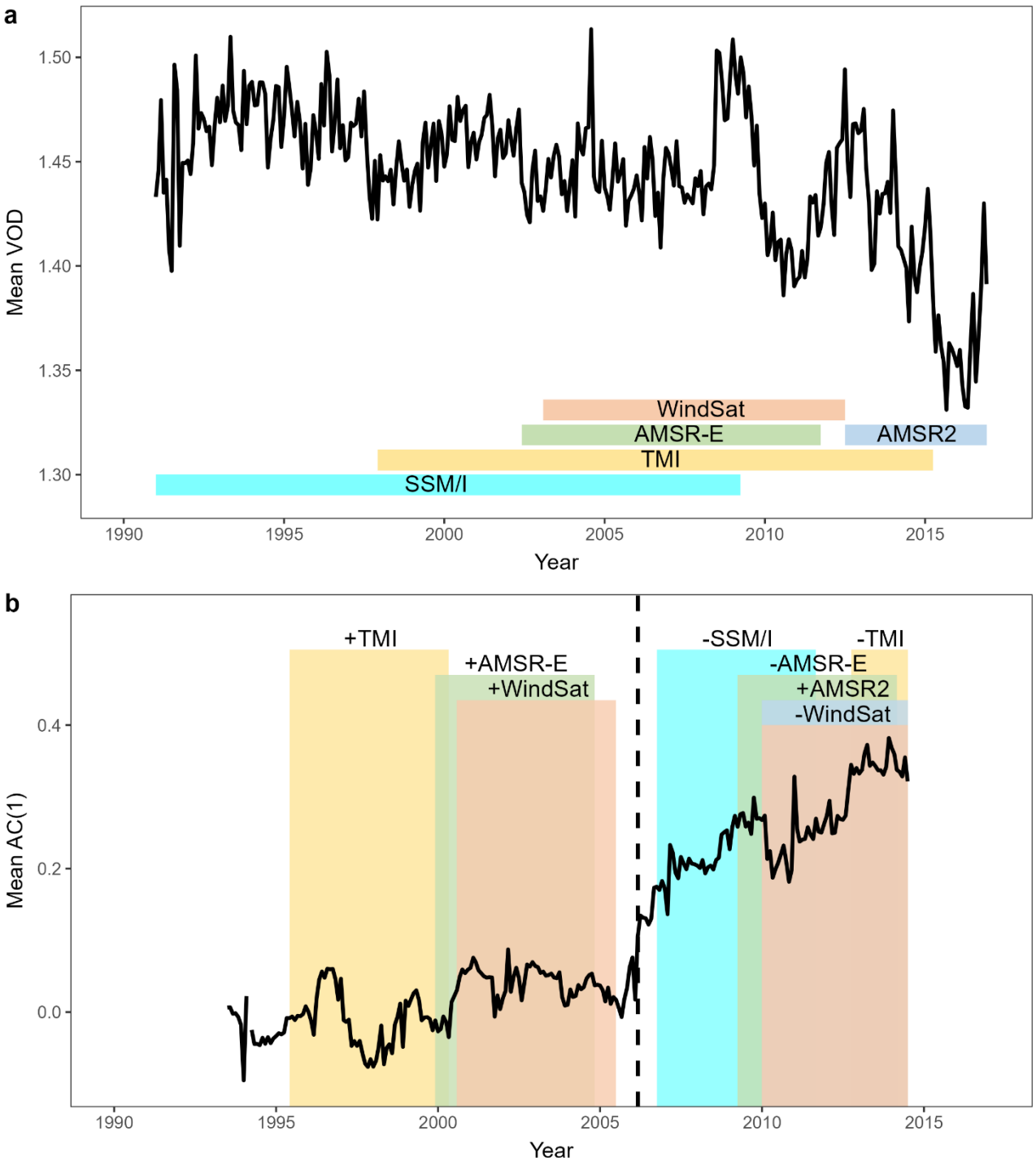

Supplementary Fig. 1 The relative time and impact of sensor shifts on time series of VOD and AC(1). a, Time series of monthly mean VOD spatially averaged over the study area, with the time span of each satellite sensor used to measure VOD shown in the bottom, adapted from Moesinger et al. (2020). **b,** Mean AC(1) time series created from mean VOD time series above, calculated on 5-year sliding windows with monthly increments and plotted at the midpoint of each window. The coloured bands correspond to the addition (+) or removal (-) of sensors and highlight sections of the AC(1) time series that were calculated on windows of VOD data that feature those particular sensor changes. The vertical dotted line indicates the breakpoint of AC(1) time series, which falls in a period where the sensor composition did not change.

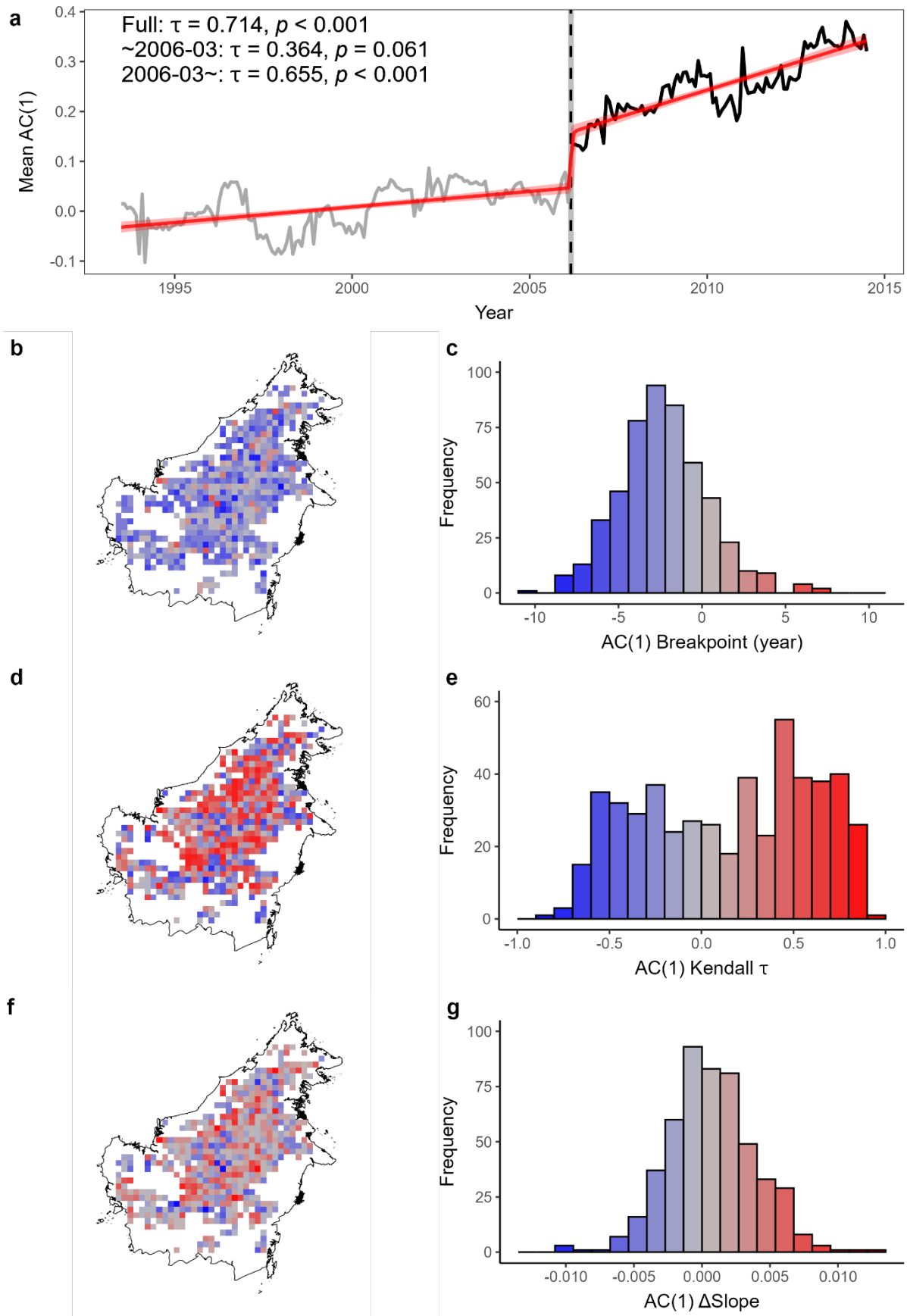

Supplementary Fig. 2 Overall trend and spatial patterns in resilience changes of Bornean rainforest when varying the threshold of evergreen broadleaf forest cover to 60% to determine study area. Recreation of **Fig. 1 (a)** and **Fig. 2 (b-g)** but using grid cells with forest cover ≥ 60%.

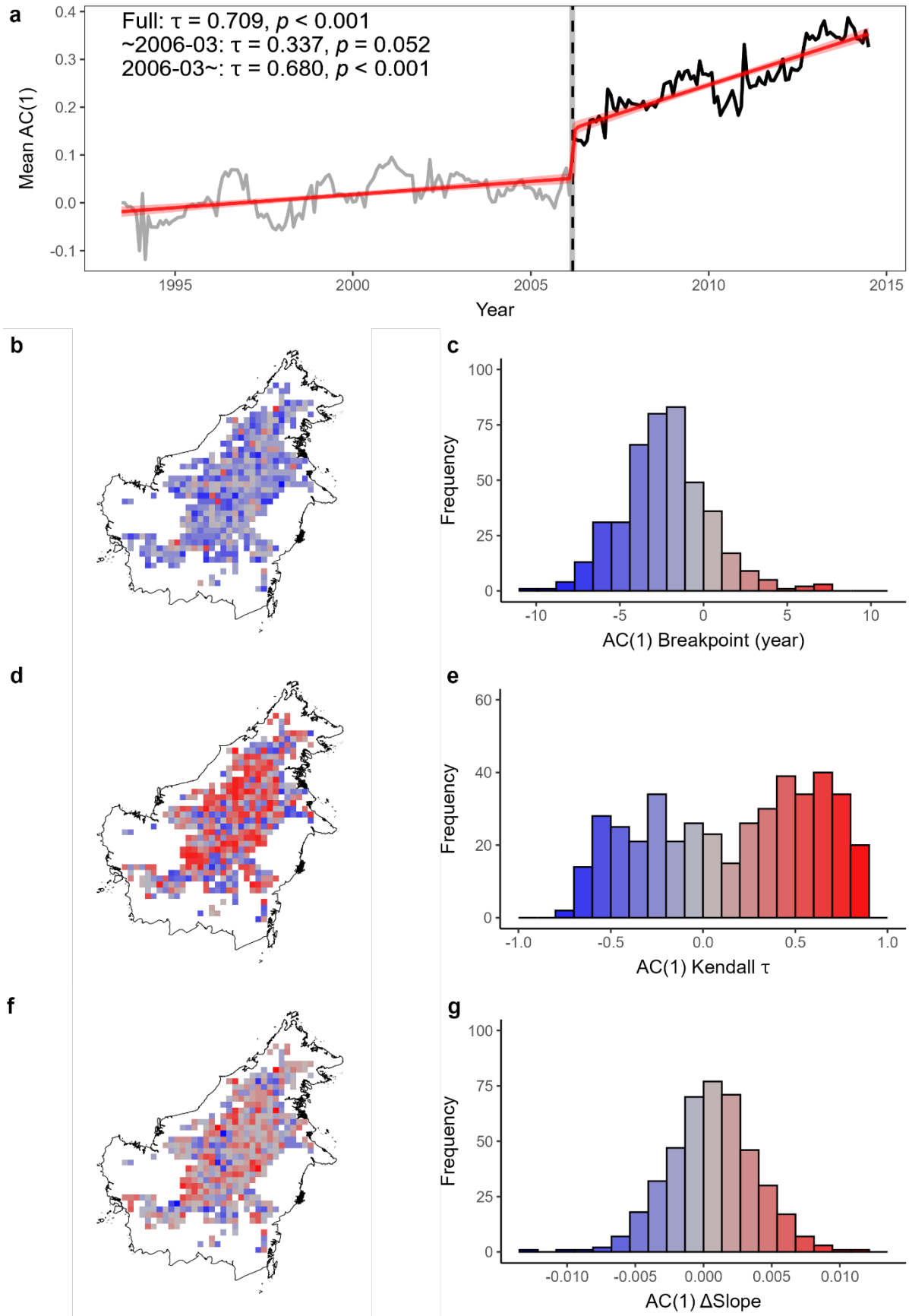

Supplementary Fig. 3 Overall trend and spatial patterns in resilience changes of Bornean rainforest when varying the threshold of evergreen broadleaf forest cover to 90% to determine study are. Recreation of **Fig. 1 (a)** and **Fig. 2 (b-g)** but using grid cells with forest cover ≥ 90%.

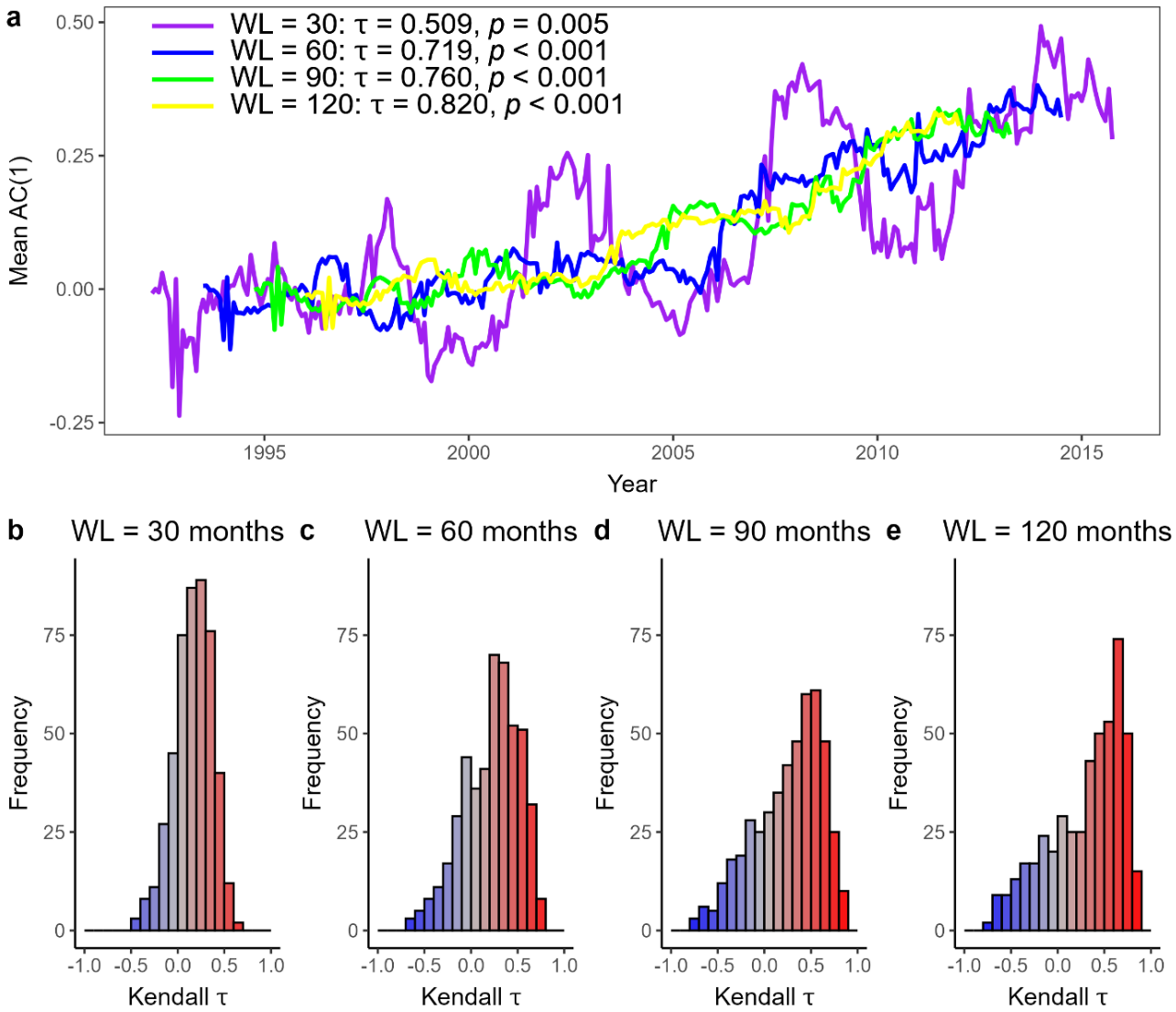

Supplementary Fig. 4 Robustness of window length to calculate VOD AC(1). a, Mean AC(1) time series when varying the window lengths of calculating to 30 months, 60 months (as in **Fig. 2d**), 90 months and 120 months. Note that the AC(1) values are plotted in the middle of the sliding window. **b-e,** Histograms of grid cells' Kendall τ values for these choices of AC(1) window lengths. WL: window length.

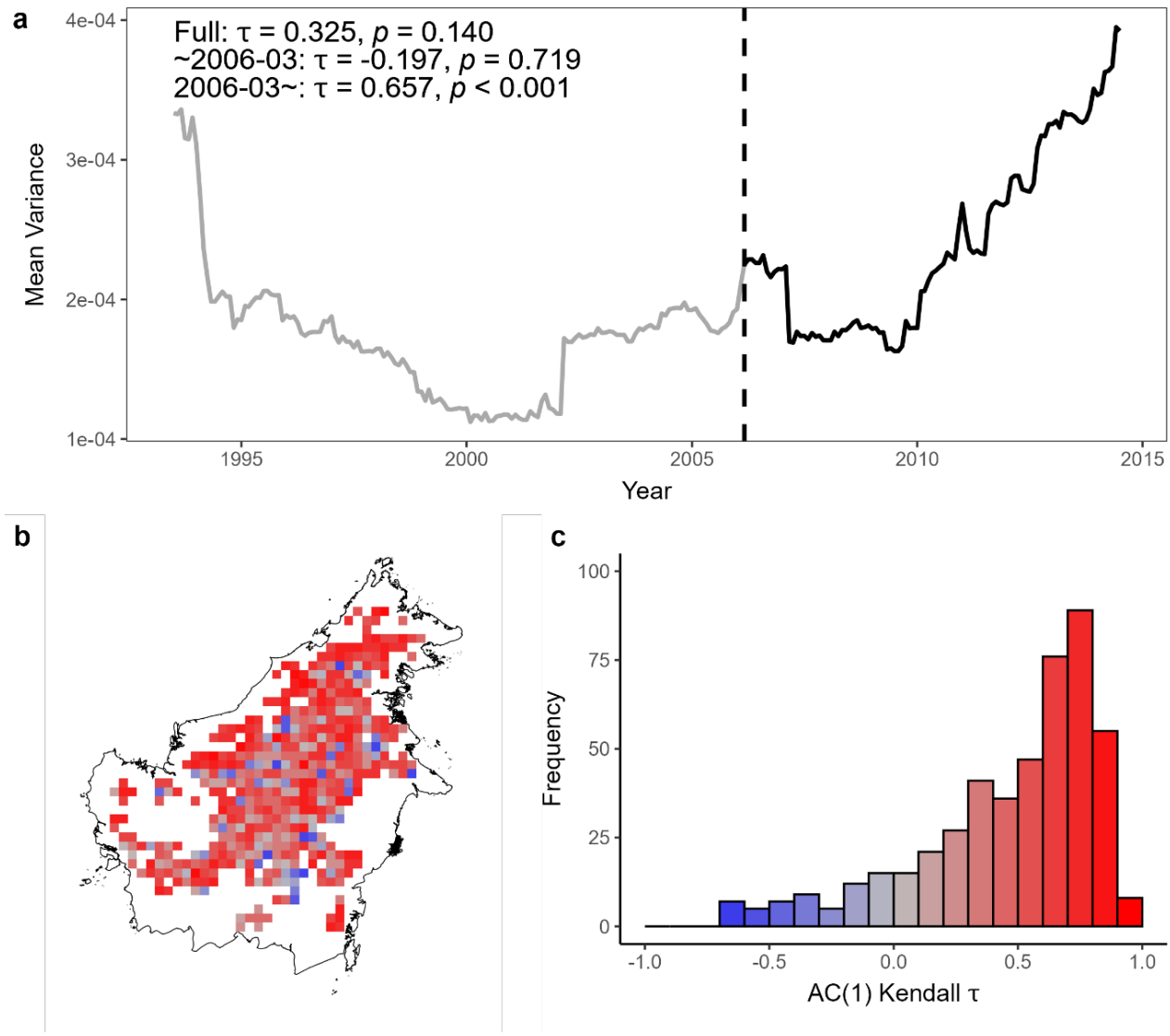

Supplementary Fig. 5 Changes in Borneo rainforest resilience since the 1990s and from the breakpoint as measured from variance of VOD. a, Mean VOD variance time series of the study area from July 1993 to July 2014 (compared to **Fig 1**). The vertical dotted line indicates the breakpoint determined from the AC(1) time series. Note that the variance values are plotted at the middle of each 5-year sliding window. **b,** Spatial distribution of Kendall *τ* values calculated from variance time series of each grid cell from 2006-03 onwards, with the same colour coding as in **c** (compared to **Fig. 2c**) **c,** Histogram of the Kendall *τ* values from 2006-03 onwards (compared to **Fig. 2d**).

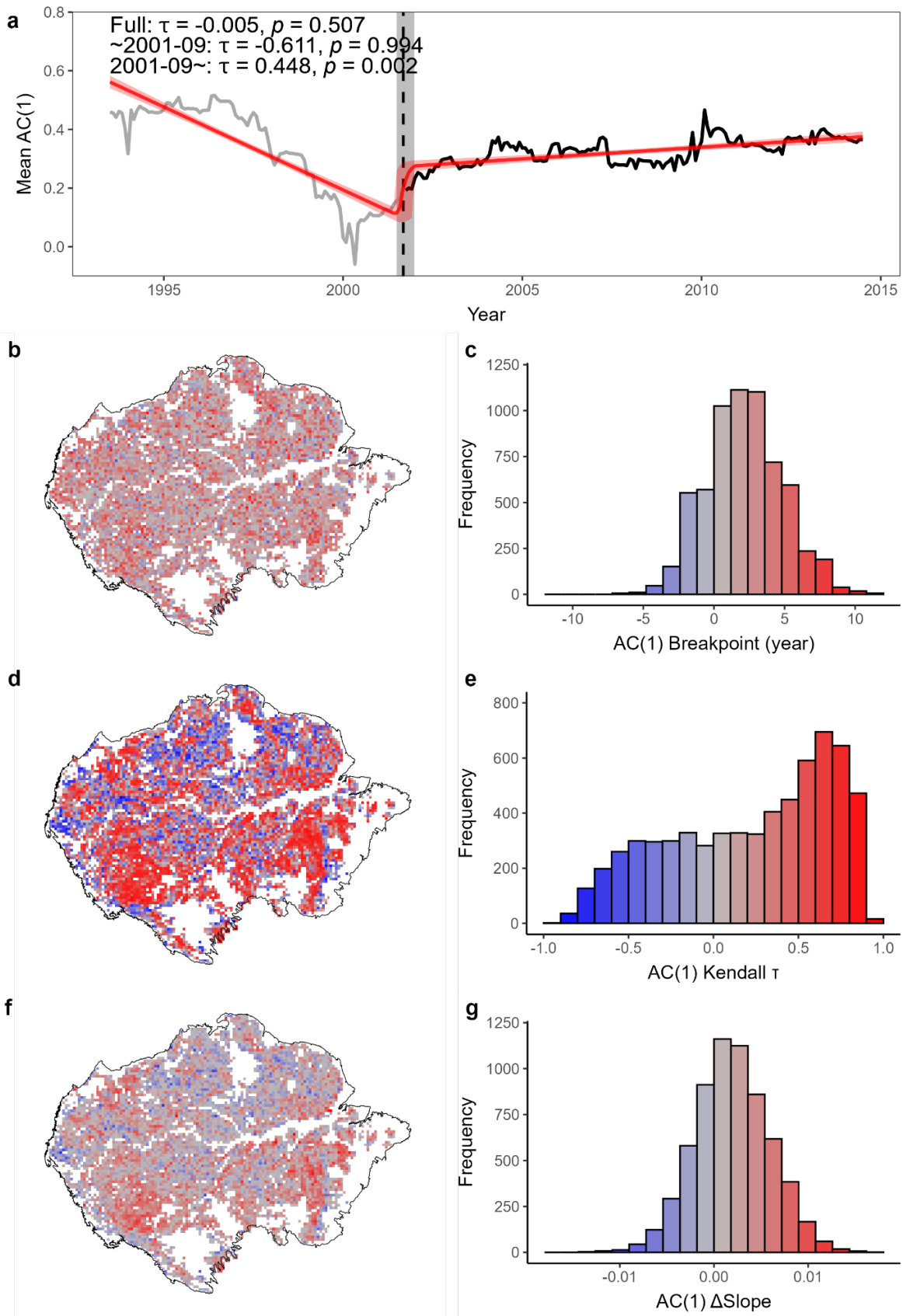

Supplementary Fig. 6 Overall trend and spatial patterns in resilience changes of Amazon rainforest, adapted from Boulton et al. (2022) with our processing pipeline. Compared to **Fig. 1 (a)** and **Figs. 2 (b-g)** but for the study area of the Amazon basin. Note that in our processing pipeline, VOD data are spatially averaged before calculating the overall mean AC(1) time series plotted in **(a)**.

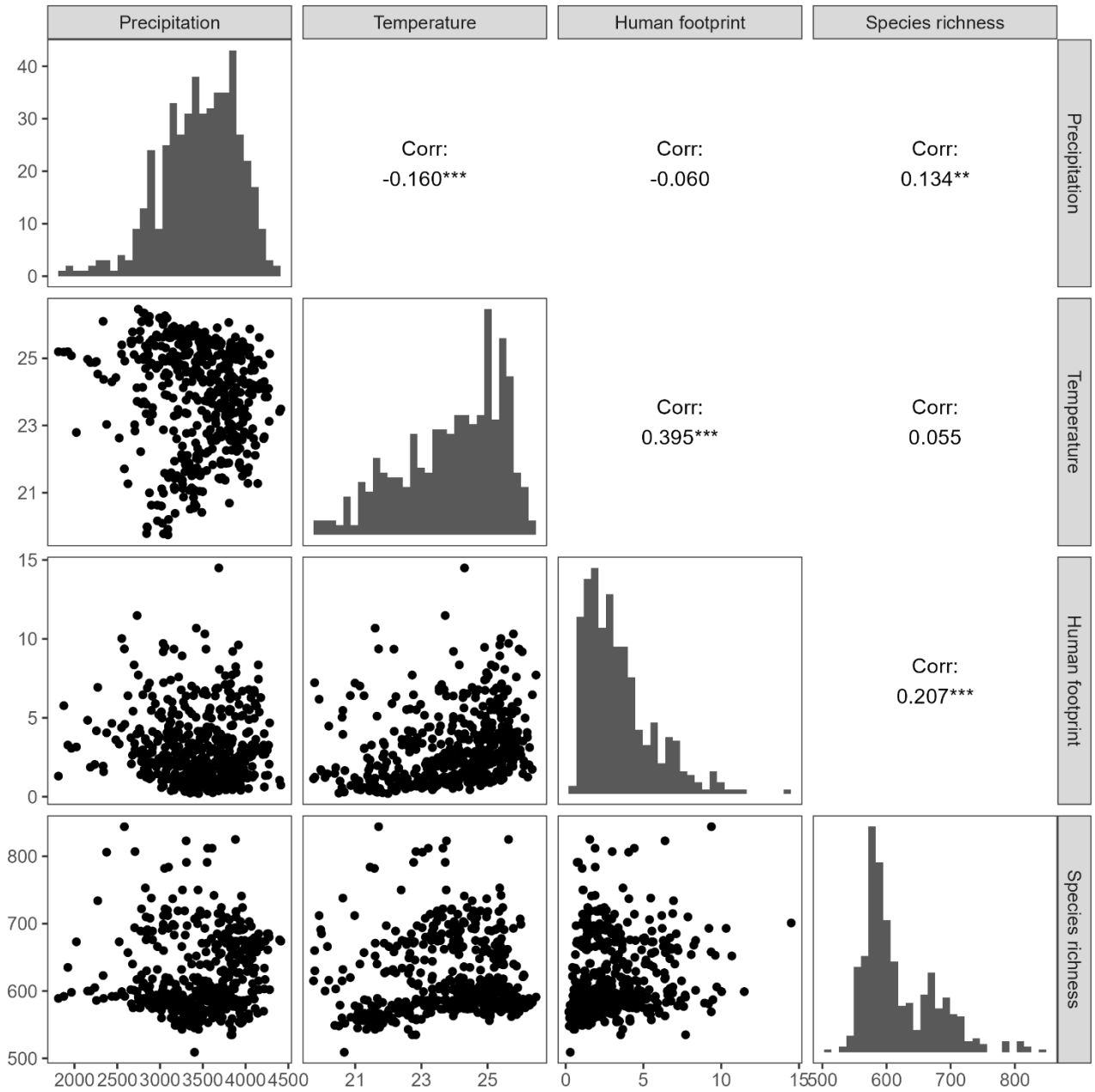

Supplementary Fig. 7 Pairwise correlations between environmental factors. The upper right panels display Spearman's correlation coefficients with significance levels (***: $p \leq 0.001$, **: $p \leq 0.01$, *: $p \leq 0.05$). The diagonal panels show histograms of each factor's distribution, while the bottom left panels present scatter plots visualizing pairwise trends.

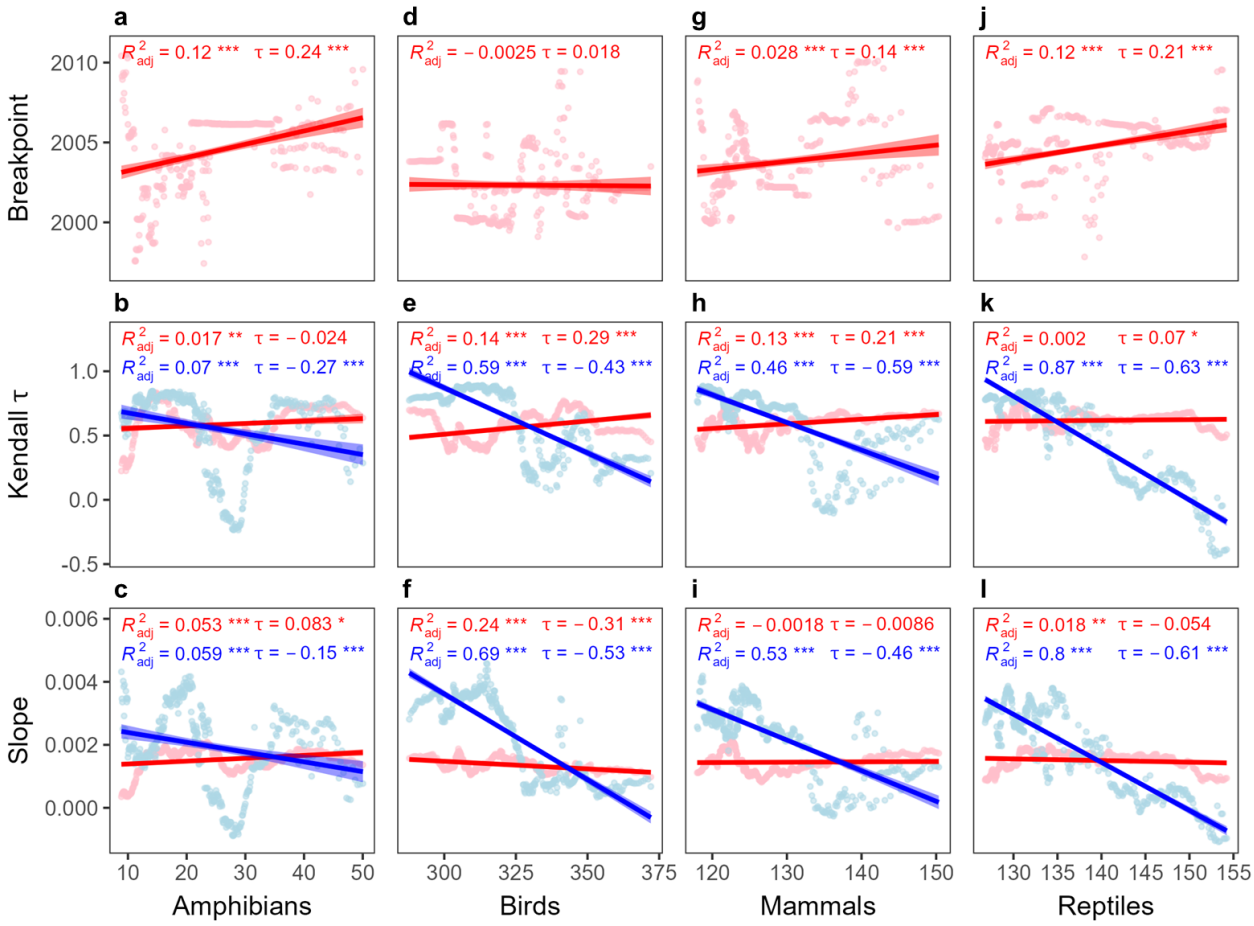

Supplementary Fig. 8 Relationship between species richness of different animal taxa and resilience (sliding band size = 100 cells). a-c, Correlation between amphibians and with resilience metrics calculated on sliding bands of grid cells along an amphibian species richness gradient (Methods): breakpoint **(a)**, Kendall τ (red: full study period; blue: post-breakpoint) **(b)** and linear regression slope (red: full study period; blue: post-breakpoint) **(c).** As in Fig. 3, we use the raw slope values rather than Δslope in order to allow comparison between the full study period and post-breakpoint period. The correlations between the resilience metrics and potential influencing factors are calculated using Kendall τ and linear models. The Kendall τ and adjusted-R^2 values are reported in each panel with their p-values denoted by stars (***: $p \leq 0.001$, **: $p \leq 0.01$, *: $p \leq 0.05$). d-l, The same as **a-c**, but for species richness gradients of birds, mammals and reptiles, respectively. In each panel, the values are plotted at the midpoint of each band.

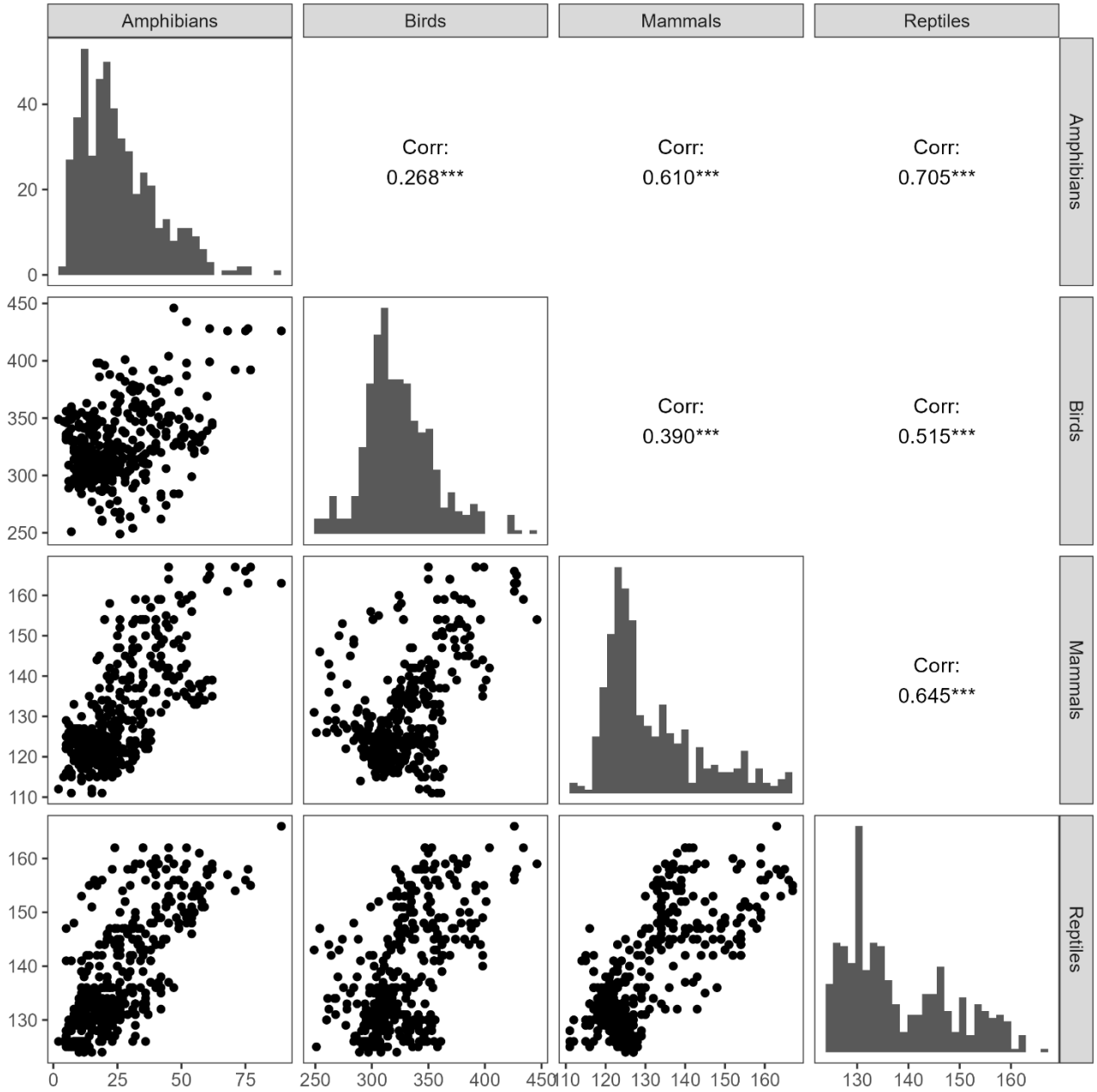

Supplementary Fig. 9 Pairwise correlations between taxa. The upper right panels display Spearman's correlation coefficients with significance levels (***: $p \leq 0.001$, **: $p \leq 0.01$, *: $p \leq 0.05$). The diagonal panels show histograms of each taxa's distribution, while the bottom left panels present scatter plots visualizing pairwise trends.

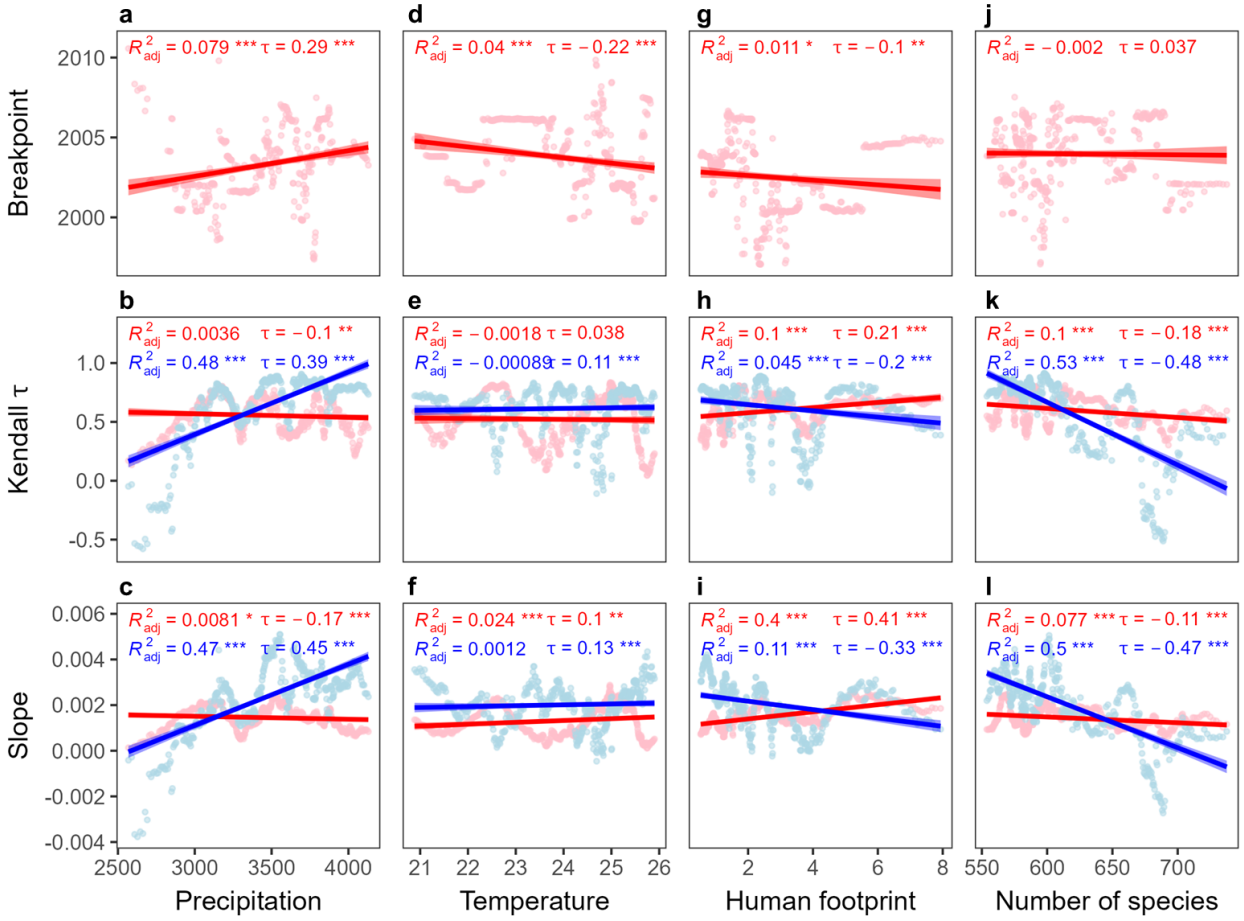

817

818 **Supplementary Fig. 10 Relationship between potential influencing factors and resilience when varying the**
819 **band size to 50 cells (recreation of Fig. 3).**

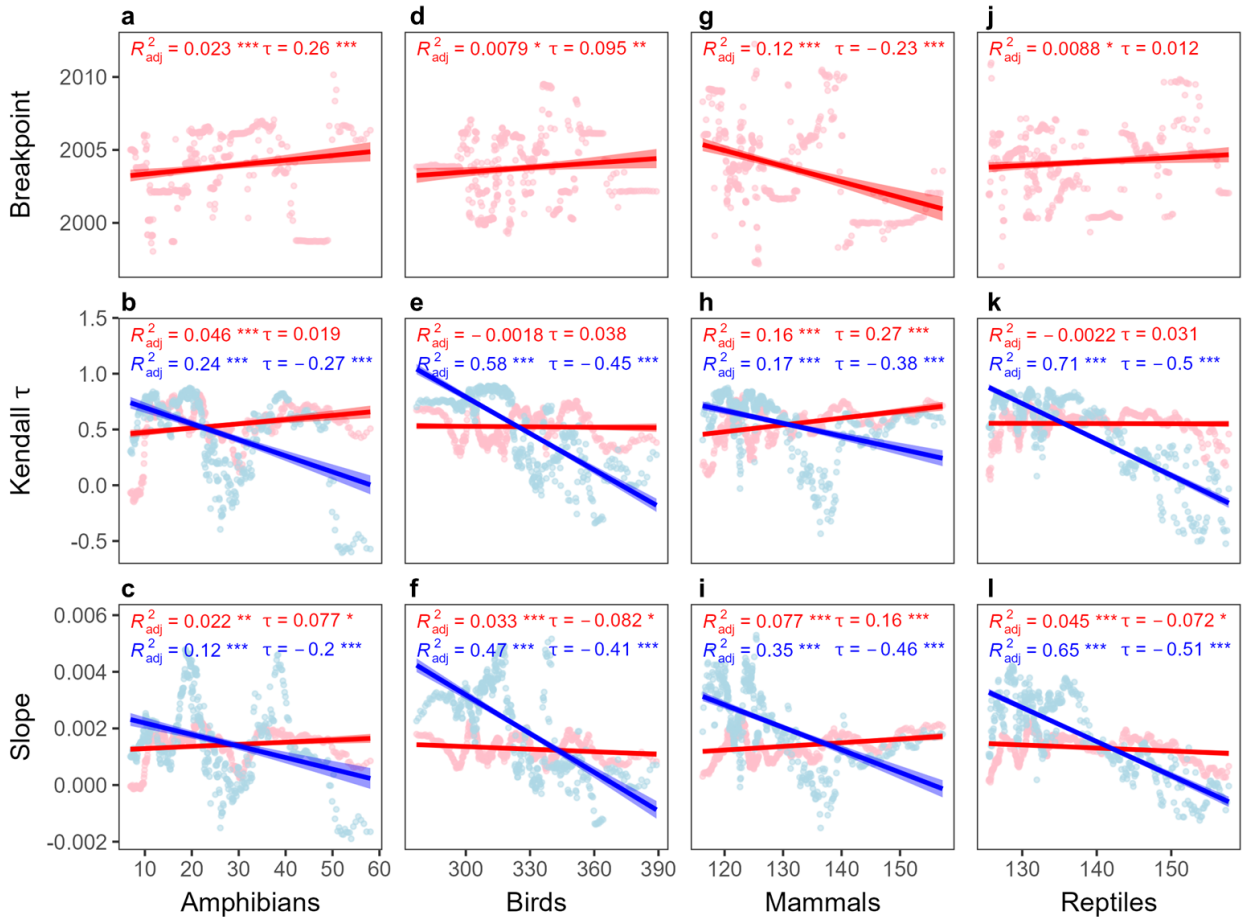

Supplementary Fig. 11 Relationship between species richness of different animal taxa and resilience when varying the band size to 50 cells (recreation of Supplementary Fig. 8).

Supplementary Table

Table S1 Coefficients and associated statistics for linear models between potential influencing factors and resilience metrics calculated on each individual grid cell.

Factor	Resilience metrics	Point Estimated	Estimate	SE	*t* value	*Pr* (>|*t*|)	Adj. R^2
Mean annual precipitation	Breakpoint	(Intercept)	$1.232*10^{4}$	$3.458*10^{2}$	35.628	< 0.001	-0.0020
		Midpoint	$2.611*10^{-2}$	$9.889*10^{-2}$	0.264	0.792	
	Kendall τ	(Intercept)	$-2.488*10^{-1}$	$1.642*10^{-1}$	-1.516	0.130	0.0103
		Midpoint	$1.143*10^{-4}$	$4.694*10^{-5}$	2.435	0.015	
	Δslope	(Intercept)	$-4.075*10^{-4}$	$1.180*10^{-3}$	-0.345	0.730	-0.0002
		Midpoint	$3.173*10^{-7}$	$3.375*10^{-7}$	0.940	0.348	
Mean annual temperature	Breakpoint	(Intercept)	13003.64	666.10	19.522	< 0.001	-0.0004
		Midpoint	-24.80	27.85	-0.891	0.374	
	Kendall τ	(Intercept)	1.47939	0.31244	4.735	< 0.001	0.0351
		Midpoint	-0.05579	0.01306	-4.272	< 0.001	
	Δslope	(Intercept)	$4.799*10^{-3}$	$2.269*10^{-3}$	2.115	0.035	0.0048
		Midpoint	$-1.720*10^{-4}$	$9.487*10^{-5}$	-1.813	0.071	
Human footprint	Breakpoint	(Intercept)	12516.61	74.38	168.274	< 0.001	0.0043
		Midpoint	-34.53	19.83	-1.741	0.082	
	Kendall τ	(Intercept)	0.152319	0.035639	4.274	< 0.001	-0.0021
		Midpoint	-0.001526	0.009503	-0.161	0.872	
	Δslope	(Intercept)	$4.736*10^{-4}$	$2.546*10^{-4}$	1.860	0.063	0.0003
		Midpoint	$7.223*10^{-5}$	$6.789*10^{-5}$	1.064	0.288	
Species richness	Breakpoint	(Intercept)	12499.9477	479.0459	26.093	< 0.001	-0.0020
		Midpoint	-0.1427	0.7709	-0.185	0.853	
	Kendall τ	(Intercept)	-0.0114981	0.2286899	-0.050	0.960	-0.0011
		Midpoint	0.0002572	0.0003680	0.699	0.485	
	Δslope	(Intercept)	$3.399*10^{-4}$	$1.636*10^{-3}$	0.208	0.836	-0.0020
		Midpoint	$5.709*10^{-7}$	$2.633*10^{-6}$	0.217	0.828	